



City Research Online

City, University of London Institutional Repository

Citation: Sriram, V. & Ma, Q. (2021). Review on the local weak form-based meshless method (MLPG): Developments and Applications in Ocean Engineering. *Applied Ocean Research*, 116, 102883. doi: 10.1016/j.apor.2021.102883

This is the accepted version of the paper.

This version of the publication may differ from the final published version.

Permanent repository link: <https://openaccess.city.ac.uk/id/eprint/27275/>

Link to published version: <https://doi.org/10.1016/j.apor.2021.102883>

Copyright: City Research Online aims to make research outputs of City, University of London available to a wider audience. Copyright and Moral Rights remain with the author(s) and/or copyright holders. URLs from City Research Online may be freely distributed and linked to.

Reuse: Copies of full items can be used for personal research or study, educational, or not-for-profit purposes without prior permission or charge. Provided that the authors, title and full bibliographic details are credited, a hyperlink and/or URL is given for the original metadata page and the content is not changed in any way.

City Research Online:

<http://openaccess.city.ac.uk/>

publications@city.ac.uk

Review on the local weak form-based meshless method (MLPG): Developments and Applications in Ocean Engineering

V. Sriram^{1*} and Q.W. Ma²

¹Associate Professor, Department of Ocean Engineering, IIT Madras, Chennai – 600 036.

²Professor, School of Engineering and Mathematical Sciences, City, University of London, UK.

*corresponding author: vsriram@iitm.ac.in

Abstract

This paper reviews the developments and applications of meshfree method based on MLPG (Meshless Local Petrov Galerkin) in ocean engineering, primarily from the work carried out at IIT Madras and City, University of London, UK. Apart from discussing the various stages in the model development, this paper will also reports its applications to small amplitude waves, wave overtopping and breaking, porous layers, long wave run-up, vegetation, floating bodies in waves, wave interaction with elastic structure and two phase flow modelling. Generally, the Navier – Stokes equation will lead to numerical dissipation for long distance propagations and increase in computational time. In order to avoid this, one needs to look for a physics based approach. One of the successfully implemented approaches in MLPG is by coupling with fully nonlinear potential flow theory (FNPT), either one-way or two-way. In this paper, we bring out the advantages and implementation issues of MLPG. [The paper also discuss the relationship with ISPH/MPS methods and some concepts that are adopted in both formulations.](#) The paper ends with the key challenges and future directions in the development of the numerical method.

Keywords: MLPG; MLPG_R; Local weak form; violent wave breaking; wave-elastic structure interactions; floating body; variable spaced approach.

1.0. Introduction

The marine structures are always exposed to severe environmental situations, which are a combination of tide, wind, current and waves. Even though all of these effects are significant, the impact of the wave is more crucial for certain structural elements. In order to understand the wave-structure interactions, experimental analysis can give convincing results, but this suffers from constraints to perform a parametric study, such as different wave parameters, water depths, the geometries of the structures, and so on. It is not practical to conduct extensive laboratory study even if the costs are of no concern. Hence, numerical simulations may be considered as a complement to experiments after sufficient validation. In numerical modelling, a physical problem will be converted to the mathematical model using the conservation principle (mass and momentum for fluid mechanics problem). Based on suitable assumptions of the considered physical problem, the mathematical model/governing equation will be simplified. The simplified form of the equation is then solved using suitable numerical algorithms through a computer

programme. In ocean engineering, two forms of governing equations or mathematical model has been employed. One based on potential flow theory and other based on Navier-Stokes (NS) Equations. In potential flow theory, fully nonlinear potential flow theory (FNPT) is preferred over the linear or weakly nonlinear theories to represent the experimental observations as close as possible. Over the past decades, the FNPT models are used for modelling wave-fixed/floating structure interaction problems (Grilli *et al.*, 2001, Ma *et al.*, 2001; Koo and Kim, 2004; Yan and Ma, 2007, Sriram *et al.*, 2006). Although the FNPT models provide better results, these models cannot deal with wave breaking and turbulence because of inviscid and irrotational assumptions. The NS models can provide a better understanding of the problems wherein viscosity and/or wave breaking need to be considered. The main disadvantage of NS models over FNPT is numerical dissipation for long time simulation and their higher computational cost. Based on the numerical methods for solving the NS equations, the numerical models are in general can be grouped into mesh-based methods and meshfree (particle) methods. In these methods, the fluid flow is based on either Lagrangian, Eulerian or Arbitrary Lagrangian-Eulerian (ALE) formulation. The traditional mesh-based methods for free surface water wave problem mainly includes Finite Difference Method (FDM, Harlow and Welch, 1965), Finite Element Method (FEM, Neuman and Witherspoon, 1970), Finite Volume Method (FVM, Hirt and Nichols, 1981) and Boundary Element Method (BEM, Nakayama and Washizu, 1981). There is a large volume of work on these methods. We will not cover the mesh-based methods here onwards in this paper.

Various meshfree methods have been developed and reported in the literature. They include Diffusion Element Method (Nayroles *et al.*, 1992), Element Free Galerkin method (EFG) (Belytschko *et al.*, 1994), Smooth Particle Hydrodynamics (Monaghan, 1988), Reproducing Kernel Particle method (Liu *et al.*, 1996), Moving Particle Semi-implicit method (Koshizuka and Oka, 1996), Meshless Local Petrov-Galerkin method (Atluri and Zhu, 1998), Particle Finite Element method (Idelsohn *et al.*, 2004). Amongst various meshfree methods, Smoothed Particle Hydrodynamics (SPH), Moving Particle Semi-implicit (MPS), Meshless Local Petrov-Galerkin (MLPG) and Particle Finite Element method (PFEM) have been widely used for solving water wave problems. Generally, these particle methods can be grouped into weakly compressible and incompressible particle method. Weakly compressible particle method solves the equation of state to estimate the pressure, whereas the incompressible particle method solves the pressure Poisson equation to calculate the pressure. Like mesh-based methods, the incompressible particle methods can be grouped into strong and weak forms. The strong-form methods include MPS and incompressible SPH (ISPH) methods. They discretise the differential equations directly and their discretisation scheme requires same order of continuity as that of the governing equations. Whereas, the weak-form methods require weaker or less continuity requirement than the original governing equations. These are further classified into global weak forms, such as PFEM, EFG and local weak forms, namely MLPG. In this paper, we restrict our discussions to the local weak form method. It should be noted that the literature on MLPG for application to solid mechanics can be referred to Atluri's and co-workers. The present paper mainly focuses on

the development in this MLPG method that was initially carried out at City, University of London and later extended both in numerical and application aspects at IIT Madras for modelling water waves and/or their interaction with structures.

2.0. History of development in MLPG for free surface waves problems

A summary of the history for the MLPG method in ocean engineering is given in Fig. 1. Atluri and Zhu (1998) were the first to propose the MLPG, and Lin and Atluri (2001) adopted this method to solve Navier-Stokes (NS) equations for the problems without free surface. In order to make the meshfree implementation simple and enhance the efficiency of the MLPG method, different mixed numerical methods in which the MLPG method combined with other numerical methods are developed. Examples are MLPG mixed finite volume method (Atluri *et al.*, 2004), MLPG mixed collocation method (Atluri *et al.*, 2006a), MLPG mixed finite difference method (Atluri *et al.*, 2006b) and so on. The MLPG approach is based on local weak form, and the local subdomain is specified for each particle. For convenience, a circle is chosen as the local subdomain for the 2D problem and a sphere for the 3D problem. The local weak form of governing equation is applied over each local subdomain. The MLPG method is truly meshless and does not need any global background mesh, either for the interpolation of test and trial function or for integrating the weak form. In the conventional Galerkin method, the test and trial functions are selected from the same functional domain, whereas in the Petrov-Galerkin method, the test and trial functions can differ. This feature makes the MLPG method highly flexible, allowing to use different test functions and formulate an easier, elegant and accurate form of equations depending upon the problem requirement.

Ma (2005a) was the first to develop the MLPG method for modelling water waves. There were two significant differences between this work and others (mentioned above). The first difference is that Ma (2005a) did not apply the MLPG concept to the whole set of equations, rather just to solving the pressure, which allows using the full Lagrangian formulation for modelling the problems with large deformations, such as nonlinear water waves. The second is to make the MLPG method to be able to deal with free surface, which other MLPG developers did not attempt at that time. In the first work, Heaviside step function was employed as the test function, which converted the equation for pressure in terms of second order derivatives into one in terms of first order derivatives. Later, Ma (2005b) and Ma (2008) modified the MLPG method to a new form called MLPG_R (Meshless Local Petrov-Galerkin method with Rankine source function) by introducing two aspects, i.e., (1) introducing the solution of Rankine source as the test function to develop the weak form over local subdomains, which produces a weak form of governing equations, that does not have the gradients of any unknown variables, improving the accuracy and robustness of the method; and (2) developing the Simplified Finite Difference Interpolation (SFDI), which are more accurate and efficient than other interpolation schemes at that times. The MLPG_R method was used by Ma and Zhou (2009) for modelling breaking waves. Further, Zhou and Ma (2010) developed a 3D version of MLPG_R method to model wave breaking and studied wave-cylinder interaction. Sriram and Ma (2010) further developed

Improved MLPG_R (IMLPG_R) method for breaking wave simulation, in which a new scheme was proposed to improve the accuracy of pressure gradient estimation.

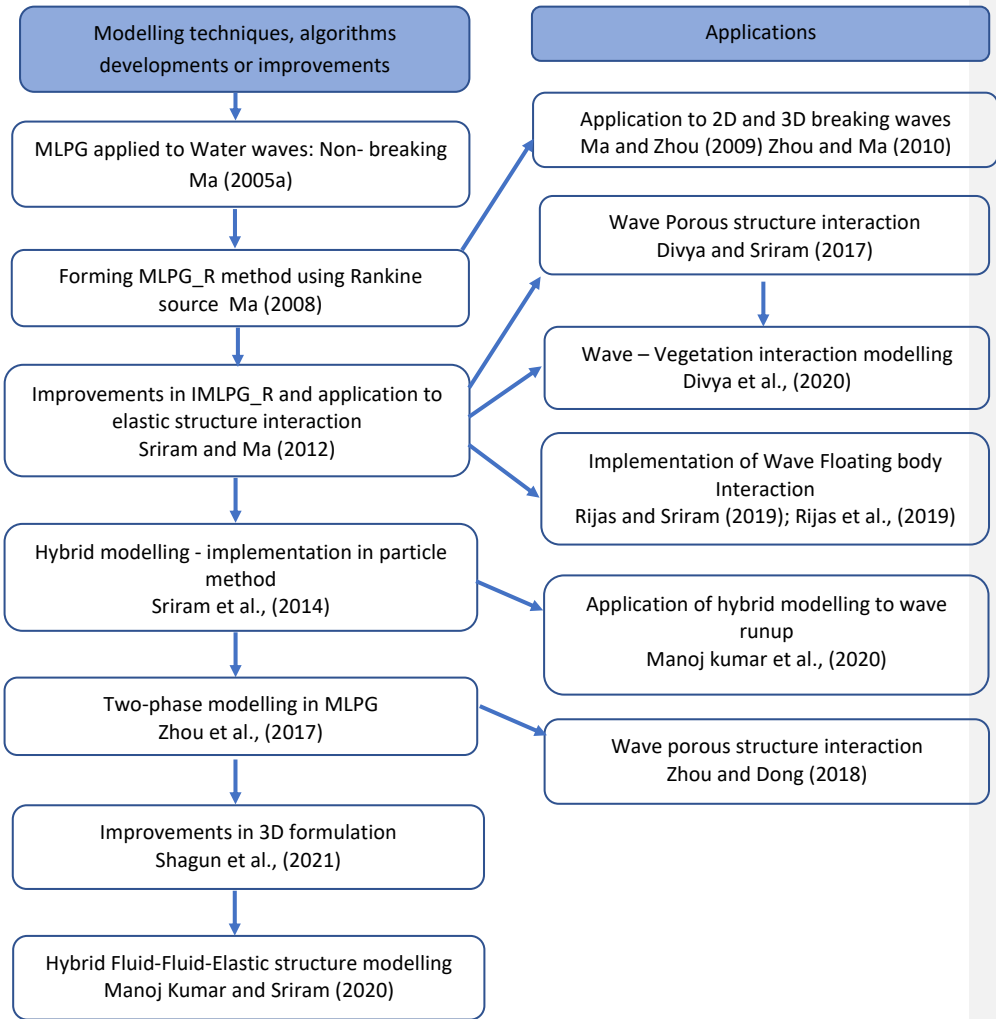


Fig.1. Summary of the history of the development of MLPG and its application in Ocean Engineering.

Sriram and Ma (2012) adopted this method to simulate violent wave interaction with elastic structures, and Divya and Sriram (2017) applied this method to model the wave interaction with porous structure. Rijas *et al.*, (2019) proposed a variable spacing approach by removing the hindrance in some of the numerical algorithms implemented in MLPG. Recently, Shagun *et al.*, (2021) proposed another major improvement in integrating the weak form using a simplified Taylor series expansion leading to symmetric form (MLPG_RS) with a quantifiable order of truncation error. A hybrid numerical model (involving different governing equations for different regions of the domain) was introduced by Sriram *et al.* (2014) to simulate non-breaking and breaking waves. In this method, the FNPT model is coupled with the NS model. This method was then extended by Manoj Kumar and Sriram (2021) for wave-elastic structure interaction problem. The MLPG_R was further developed by Zhou *et al.*, (2017) to deal with two-phase problems with or without breaking interface. The sharp interface algorithm proposed by Zhou *et al.*, (2017) was adopted for wave porous modelling in Zhou and Dong (2018).

Overall, the concept of MLPG has been developed and improved pertaining to ocean engineering applications in the past 15 years, as shown in Fig. 1. However, there was no review articles on this overall development and different applications of the method, compared to several review articles on other class of particle methods, such as Monaghan (2012); Violeau and Rogers (2016), Gotoh and Khayyer (2018), Ye *et al.*, (2019), Vacondio *et al.*, (2020), Lind *et al.*, (2020). In the subsequent sections, we will discuss the numerical approaches, algorithms and implementation strategies, and the various applications in ocean engineering, ranging from wave overtopping, long wave runup, breaking waves, porous structure, vegetation interactions, elastic structure interactions, multiphase problem and floating body. [Apart from reporting the developments in MLPG, the paper will discuss the similarities and differences between the MLPG and ISPH. So, the state of art the concepts adopted in SPH can be taken forward to MLPG or vice versa. Finally, the paper ends with the future directions for the MLPG development and scope for adopting concepts from SPH .](#)

3.0 Relationship between MLPG and ISPH/MPS

MLPG method was adopted for the incompressible fluid by solving pressure Poisson Equation (PPE) based on Chorin's projection scheme, hence the SPH version (namely, ISPH) and MPS was reviewed in this article to show the relationships between the two approaches. The pioneering particle method that adopts this strategy in strong form is MPS proposed by Koshizuka *et al.*, (1995) for free surface waves. In SPH, Lo and Shao (2002) applied this projection framework for free surface waves. There are two types of boundary conditions in solving the BVP, one on the free surface (both kinematic and dynamic) and [the other on the solid body boundary conditions. Again, the](#) The free surface identification can be thought of similar between MLPG and ISPH, even though different approaches and combinations are adopted as discussed in Section. 4.6. The other algorithms, such as gradient estimations, Laplacian

operator and particle shifting can be interchanged between MLPG and ISPH/MPS. The deviations and similarities of the ideas between the MLPG and ISPH/MPS are shown in Fig.1. The figure clearly shows the deviations and the similarities that exist between SPH and MLPG. Because of this, hence Zheng et al. (2014) modified the PPE using MLPG concept and proposed ISPH_R method, keeping all the algorithms/procedure same. They have shown that by doing so, it requires very less number of nodes with improved accuracy compared to traditional ISPH and other variants of ISPH. The green color box in Fig.2 represents the discretisation terms aspects, wherein one can employ same procedure in MLPG and ISPH/MPS. However, some modifications and new approaches have been used in MLPG, as discussed later. The implementation of boundary condition is different in MLPG compared to ISPH/MPS, a detailed discussion on this aspect and the treatment of boundary conditions in MLPG and comparison of similar implementation as in ISPH/MPS whilst solving PPE was reported by Zhou et al., (2008). It was reported that a detailed study on the implementation of solid boundary conditions treatments in the way as in ISPH/MPS could lead to noisy pressure fluctuations in MLPG was reported. Further, it is interesting to point out that in the MLPG, if one chooses the test function as Kronecker delta property, it leads to collocation approach (as discussed by Atluri and Shen, 2002). In the collocation approach, adopting the interpolation scheme such as Simplified Finite Difference scheme, the special forms lead to MPS (See Ma, 2005a for derivation). Alternatively, using Heaviside step function one can show mathematically that the MLPG formulation leads to standard MPS. This will be derived in next section.

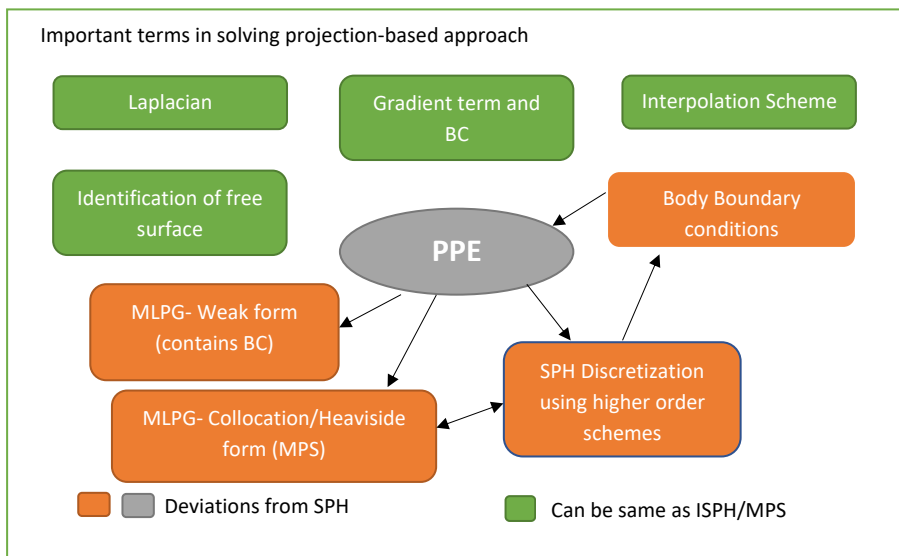


Fig.2 The similarities and deviations in comparison between ISPH/MPS and MLPG concept of solving using projection based approach.

4.0. Stages in Numerical Model Development

The development of MLPG for ocean engineering applications can be grouped into (a) wave-rigid structure interactions, this includes wave overtopping, runup, nonlinear wave-wave interactions with structure, violent wave impacts; (b) Wave-porous structure interactions or vegetation interactions, wherein governing equations need to be suitably changed and numerical algorithms need to be implemented properly (c) Incorporating variable spacing to handle floating body (d) Wave-elastic structure interactions, particularly to address small amplitude and violent waves; and (e) two-phase modelling, wherein treatment of sharp interface is required. Based on the above aspects, the technical aspects of the numerical schemes need to be developed. These are addressed in the below section [with the exchange of concepts between MLPG and other particle methods](#).

4.1. Governing equations (Single phase) and modelling approach for Wave-Structure Interaction

The governing equations used for solving the incompressible fluid domain for wave-structure interaction are continuity and momentum equations, which are given by,

$$\nabla \cdot \vec{u} = 0 \quad (1)$$

$$\frac{D\vec{u}}{Dt} = -\frac{1}{\rho} \nabla p + \vec{g} + \nu \nabla^2 \vec{u} \quad (2)$$

where \vec{u} is the fluid velocity vector, ρ is the fluid density, p is the fluid pressure, \vec{g} is the gravitational acceleration and ν is the kinematic viscosity of the fluid.

The free surface is governed by two boundary conditions, namely, kinematic and dynamic. The Lagrangian form of kinematic and dynamic free surface boundary conditions are expressed as,

$$\frac{D\vec{r}}{Dt} = \vec{u} \quad (3)$$

$$p = 0 \quad (4)$$

where \vec{r} is the position vector. The solid walls, including floating body surface should satisfy the following conditions,

$$\vec{u} \cdot \vec{n} = \vec{U} \cdot \vec{n} \quad (5)$$

$$\vec{n} \cdot \nabla p = \rho \left(\vec{n} \cdot \vec{g} - \vec{n} \cdot \vec{U} + \nu \vec{n} \cdot \nabla^2 \vec{u} \right) \quad (6)$$

where \vec{n} is the unit normal vector of the solid boundary, \vec{U} and $\vec{\dot{U}}$ are the velocity and acceleration vectors of the solid walls, respectively. For most of the applications in ocean engineering, the slip boundary condition (Eq. ~~(5)~~(5)) has been imposed on the wall boundaries. This is because the no-slip boundary condition requires to resolve the rapid change of tangential velocity near the walls, which needs fine particle resolution and leads to high computation costs without significant gain in accuracy of the results. In some problems associated with wave-structure interaction, the no-slip boundary condition may need to be considered (Rijas *et al.*, 2019).

The governing equations ~~(1)~~(4) & ~~(2)~~(2) are solved by using the mesh-free method with fractional time-split algorithm introduced by Chorin (1968). It starts from a particular instant (n^{th} time step) in which the pressure, velocity and position of particles are known. The physical quantities for $(n+1)^{\text{th}}$ time step are updated by solving governing equations as given below.

- i. Explicitly find out the intermediate velocity \vec{u}^* and position \vec{r}^* of the particles using

$$\vec{u}^* = \vec{u}^n + \vec{g}\Delta t + \nu \nabla^2 \vec{u}^n \Delta t \quad (7)$$

$$\vec{r}^* = \vec{r}^n + \vec{u}^* \Delta t \quad (8)$$

where superscript n denotes n^{th} time step, and Δt is the time step size. Laplacian operator derived by Koshizuka *et al.* (1998) is used to estimate $\nabla^2 \vec{u}$ in Eq. ~~(7)~~(7).

- ii. Implicitly evaluate pressure p^{n+1} from the pressure Poisson equation given by:

$$\nabla^2 p^{n+1} = \alpha \frac{\rho^{n+1} - \rho^*}{\Delta t^2} + (1 - \alpha) \frac{\rho}{\Delta t} \nabla \cdot \vec{u}^* \quad (9)$$

where ' α ' is an artificial coefficient with value lies between 0 and 1; ρ^{n+1} and ρ^* is the fluid density at $(n+1)^{\text{th}}$ time step and intermediate time step, respectively. Update the fluid particle velocity and position at $(n+1)^{\text{th}}$ time step using

$$\vec{u}^{n+1} = \vec{u}^* - \frac{\Delta t}{\rho} \nabla p^{n+1} \quad (10)$$

$$\vec{r}^{n+1} = \vec{r}^* + \vec{u}^{n+1} \Delta t \quad (11)$$

- iii. Go to next time step.

In the above procedure, adaptation of Eq. (9)(9) in MLPG need to be discussed. Ma (2005) taken α as zero, this was adopted by most of the global weak formulation based approach. Later, Zhou and Ma (2009), whilst testing for breaking wave applications, noticed that the nodes were segregated in some locations and coarse at other locations, particularly near the trough or near boundaries and introduced α as 0.1-0.2. Later, this problem was investigated in detail by Sriram and Ma (2010), and indicated that it would be better to take α as zero with improvement of the method in other aspects. Hence, in the subsequent work, the value of ' α ' is taken as zero, such as particle shifting technique proposed in Sriram and Ma (2012).

In the numerical algorithm described above the key task is to solve the Pressure Poisson Equation (PPE) given in Eq. (9)(9). Either strong forms, global or local weak forms may be used. The MLPG_R method will be summarised, which discretises the computational domain into randomly distributed particles or nodes as given in Fig.3. The particles are separated into three main categories, i.e., the inner particles, the free surface particles and wall particles (particles present on the rigid boundaries). Each particle I in the domain is enclosed by a sub-domain Ω_I centred at the node itself, having radius R_I . The sub-domain is a circle for the 2D and a sphere for the 3D problem.

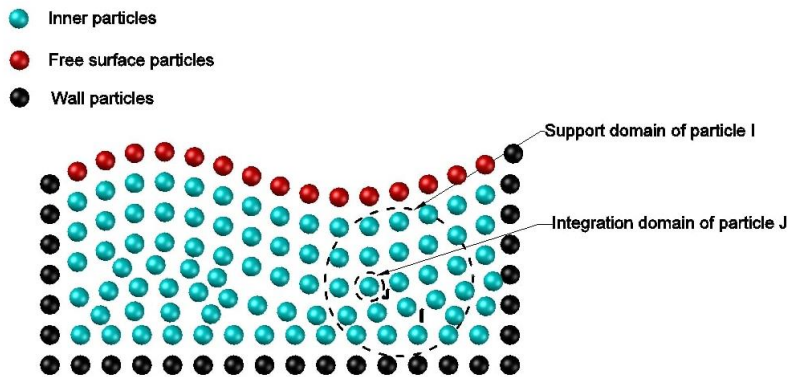


Fig. 3. Illustration of particles, support domain and integration domain in MLPG (2D - Circle and 3D - Sphere)

4.1.1. Integration form of PPE and its relationship to MPS and ISPH

The weak form of Eq. (12)(12) is obtained by multiplying it with an arbitrary test function ϕ and integrating over the circular sub-domain of each particle.

Formatted: Font color: Auto

$$\int_{\Omega_I} \left[\nabla^2 p^{n+1} - (1 - \alpha) \frac{\rho}{\Delta t} \nabla \cdot \vec{u}^* - \alpha \frac{\rho^{n+1} - \rho^*}{\Delta t^2} \right] \varphi d\Omega = 0 \quad (12)$$

The above equation is normally called as Local Unsymmetric Weak Form (LUWF). The concept of the MLPG method is the flexibility in selecting different test functions, leading to different formulations.

After applying Heaviside test function (i.e. 1 inside the domain and 0 otherwise), Eq. (12) becomes

$$\int_{\Omega_I} \nabla^2 p^{n+1} d\Omega = \int_{\Omega_I} \left[(1 - \alpha) \frac{\rho}{\Delta t} \nabla \cdot \vec{u}^* \right] d\Omega + \int_{\Omega_I} \left[\alpha \frac{\rho^{n+1} - \rho^*}{\Delta t^2} \right] d\Omega \quad (13)$$

Applying Gauss theorem for the left hand side and 1st term in right hand side and applying particle number density approximation to the last term leads to:

$$\int_{\partial\Omega_I} \vec{n} \cdot \nabla p^{n+1} dS = (1 - \alpha) \frac{\rho}{\Delta t} \int_{\partial\Omega_I} \vec{n} \cdot \vec{u}^* dS + \alpha \frac{\rho}{n_0 \Delta t} \left(\frac{Dn}{Dt} \right)^* \quad (14)$$

For a circular local domain (Ω_I) in 2D cases, the above equation is

$$\int_{\partial\Omega_I} \frac{\partial p^{n+1}}{\partial r} dl = (1 - \alpha) \frac{\rho}{\Delta t} \int_{\partial\Omega_I} \vec{n} \cdot (\vec{u}^* - \vec{u}_I^*) dl + \alpha \frac{\rho}{n_0 \Delta t} \left(\frac{Dn}{Dt} \right)^* \quad (15)$$

where dl is the segment arc length of the circular domain. The subscript I denotes the center of Ω . Using the mathematical derivation to obtain the standard MPS scheme provided by Isshiki (2011) and subsequently used by Ng *et al.*, (2014), the final form can be obtained.

$$\int_{\partial\Omega_I} \frac{\partial p^{n+1}}{\partial r} dl = \frac{2d}{n_i} \frac{\sum_{j \neq i} (p_j - p_i) w(|\vec{r}_j - \vec{r}_i|)}{(\sum_{j \neq i} w(|\vec{r}_j - \vec{r}_i|))^{-1} \sum_{j \neq i} |\vec{r}_j - \vec{r}_i|^2 w(|\vec{r}_j - \vec{r}_i|)} = \langle \nabla^2 p^{n+1} \rangle \quad (16)$$

$$\int_{\partial\Omega_I} \vec{n} \cdot (\vec{u}^* - \vec{u}_I^*) dl = \frac{2d}{n_i} \sum_{j \neq i} \frac{(\vec{u}_j^* - \vec{u}_i^*)}{|\vec{r}_j - \vec{r}_i|^2} (\vec{r}_j - \vec{r}_i) w(|\vec{r}_j - \vec{r}_i|) \quad (17)$$

Thus, this shows that the MPS can be considered as one of the variants of the MLPG by adopting the test function suitably, though they have been developed parallelly. The order of consistency with the MPS standard form is $O(R_1^2)$. R_1 corresponds to radius of the support domain. Having

established the relationship between MPS and MLPG, the relationship between MPS and ISPH has already been rigorously established (see Souto-Iglesias et al., 2013, 2014). The improvements of both MPS and ISPH are reviewed extensively (Li et al., Luo et al., 2021) and will not be repeated here. Many improvements have been proposed for Eqn. (16) and (17) by employing higher order schemes (Gotoh and Khayyer, 2016). Using the two equations, Eqn. 15 can be rewritten in the matrix form, which is similar to one of numerical form of MLPG method shown later.

$$[K_{IJ}] \cdot \{P\} = [B_I] \quad (18)$$

$$K_{IJ} = \begin{cases} \frac{2d}{n_i} \frac{\sum_{j \neq i} w(|\vec{r}_j - \vec{r}_i|)}{(\sum_{j \neq i} w(|\vec{r}_j - \vec{r}_i|))^{-1} \sum_{j \neq i} |\vec{r}_j - \vec{r}_i|^2 w(|\vec{r}_j - \vec{r}_i|)} & \text{for Inner fluid particle} \\ \nabla \phi & \text{for particles on solid boundary} \end{cases} \quad (18a)$$

$$B_I = \begin{cases} (1 - \alpha) \frac{\rho}{\Delta t} \nabla \cdot \vec{u}^* + \alpha \frac{\rho}{n_0 \Delta t} \left(\frac{Dn}{Dt} \right)^* & \text{for Inner fluid Particle} \\ \frac{\rho}{\Delta t} \vec{n} \cdot (\vec{u}^* - \vec{U}^{n+1}) & \text{for solid boundary particle} \\ P_{atm} & \text{for free surface particle} \end{cases} \quad (18b)$$

Similarly, the standard ISHP can be written in the matrix form as (Zheng et al., 2014)

$$K_{IJ} = \begin{cases} \sum_{j \neq i} 2 \frac{m_j}{\rho_j} \frac{\vec{r}_{ij}^k w_{jk}}{|\vec{r}_j - \vec{r}_i|^2 + \delta^2} & \text{for Inner fluid particle} \\ \nabla \phi & \text{for particles on solid boundary} \end{cases} \quad (19a)$$

$$B_I = \begin{cases} (1 - \alpha) \frac{\rho}{\Delta t} \nabla \cdot \vec{u}^* + \alpha \frac{\rho^{n+1} - \rho^*}{\Delta t^2} & \text{for Inner fluid Particle} \\ \frac{\rho}{\Delta t} \vec{n} \cdot (\vec{u}^* - \vec{U}^{n+1}) & \text{for solid boundary particle} \\ P_{atm} & \text{for free surface particle} \end{cases} \quad (19b)$$

where m is the mass of the particle in SPH, $W_{,k}$ is the partial derivative of the kernel function with respect to the coordinate in k direction. ϕ is the shape function depending on the meshfree interpolation scheme for gradient estimation at the boundary, such as MLS.

The above formulations are rooted to Eq. (15), which involves the approximation to the derivative of unknown function, i.e., pressure in this case.

It is well known that it is better to use a formulation without involvement of any derivatives. This is due to the fact that the numerical approximation of derivatives, particularly the second order derivatives will lead to inconsistency and so larger error, more evidently for free surface waves problems that often involve the random distribution of particles. Before Ma (2005b), the best formulation has involved the first order derivatives in the transformed governing equation. It is the paper of Ma (2005b) that proposed a formulation without involving any derivatives of any unknown functions and named as MLPG_R method. This paper used Rankine source solution as the test function. Such test function ϕ satisfies $\nabla^2\phi = 0$ in the domain Ω_l except at its centre and $\phi = 0$ on its boundary $\partial\Omega_l$. The expression of the test function based on the Rankine source solution for 2D is

$$\phi = \frac{1}{2\pi} \ln\left(\frac{r}{R_l}\right) \quad (20)$$

where r is the distance between concerned particle in the domain and the centre of Ω_l . The test function for 3D,

$$\phi = \frac{1}{4\pi} \left(1 - \frac{R_l}{r}\right) \quad (21)$$

With such a test function, Eq. ~~(12)~~(12) is transformed into a new form considering $\alpha = 0$, which (as in Ma, 2009) for 2D is

$$\int_{\partial\Omega_l} n \cdot (p\nabla\phi) ds - p = \int_{\Omega_l} \frac{\rho}{\Delta t} \bar{u}^* \cdot \nabla\phi d\Omega \quad (22)$$

And for 3D, it becomes

$$\int_{\partial\Omega_l} n \cdot (p\nabla\phi) ds - R_l p = \int_{\Omega_l} \frac{\rho}{\Delta t} \bar{u}^* \cdot \nabla\phi d\Omega \quad (23)$$

As one can see, Eqs. ~~(22)~~(22) and (23) do not have derivatives of the pressure and velocity (unknown variables to be solved). As such the approximation to the unknown functions in the equations just need their existence but do not require any continuous derivatives. In contrast, approximation to the unknown functions in Eq. ~~(12)~~(12) needs them to have finite or at least integrated second-order derivatives. Therefore, the use of Eqs. ~~(22)~~(22) or (23) for further

Formatted: Font color: Text 1

Formatted: Font: (Asian)+Body Asian (DengXian)

Formatted: Font color: Text 1

Formatted: Font: (Asian)+Body Asian (DengXian)

discretisation has a tremendous numerical advantage over the use of Eq. ~~(12)(12)~~ directly. It is noted that the ~~IMP~~SPS (or ISPH) method (the later discretising Eq. ~~(12)(12)~~ directly) requires higher-order approximation (as discussed by Lind et al., 2020, and Ma et al., 2016), compared with the MLPG_R method, other schemes are quite similar between them.

Formatted: Font color: Text 1

Formatted: Font color: Text 1

Eq. ~~(6)(6)~~ is used to impose the condition for pressure on solid boundaries. This equation contains the term $\nabla^2 \vec{u}$, which demands estimating the second-order derivative at the rigid boundary. Although the calculation of $\nabla^2 \vec{u}$ is not a difficult task, suppressing the error associated is not easy in computational practice as the fluid particles situated only on one side of the boundary. Hence, it is better to avoid the computation of the second-order derivatives, if possible. So, Eq. ~~(5)(5)~~ combined with Eq. ~~(10)(10)~~ to form an alternate equation for the solution of pressure on the solid boundaries in Zhu and Ma (2009) as follows,

$$\vec{n} \cdot \nabla p^{n+1} = \frac{\rho}{\Delta t} \vec{n} \cdot (\vec{u}^* - \vec{U}^{n+1}) \quad (24)$$

where \vec{u}^* calculated from Eq. ~~(7)(7)~~ by substituting \vec{u}^n with \vec{U}^n . For fixed solid boundaries, $\vec{n} \cdot \vec{U}^{n+1} = 0$. Even though $\nabla^2 \vec{u}$ is solved in Eq. ~~(7)(7)~~ to estimate \vec{u}^* , the second-order term is not explicitly involved in Eq. ~~(24)(24)~~ and no need to calculate it again once \vec{u}^* is calculated. The summary about the discretization of Eq. ~~(22)(22)~~ and associated boundary conditions is given below for completeness. More details may be found in Ma (2005b, 2008) and Ma and Zhou (2009).

Formatted: Font: (Asian) +Body (Calibri), Check spelling and grammar

$$[K_{II}][\hat{p}] = [B_I] \quad (25)$$

For 2D:

$$K_{II} = \begin{cases} \int_{\partial\Omega_f} \Phi_J(\vec{x}) n \cdot \nabla \varphi ds - \Phi_J(\vec{x}) & \text{for water nodes} \\ n \cdot \nabla \Phi_J(\vec{x}) & \text{for solid boundary nodes} \end{cases} \quad (26a)$$

For 3D:

$$K_{II} = \int_{\partial\Omega_f} \Phi_J(\vec{x}) n \cdot \nabla \varphi ds - R_I \Phi_J(\vec{x}) \quad \text{for water nodes} \quad (26b)$$

and (for both 3D and 2D)

$$B_I = \begin{cases} \int_{\Omega_f} \frac{\rho}{\Delta t} \vec{u}^* \cdot \nabla \varphi d\Omega & \text{for water nodes} \\ \frac{\rho}{\Delta t} \vec{n} \cdot (\vec{u}^* - \vec{U}^{n+1}) & \end{cases} \quad (27)$$

for solid boundary nodes

In the equations, the integration on the right side is performed by the semi-analytical method discussed in Ma (2008).

Although the computational models for simulating fluid flows are based on the conservation of mass and momentum equations, the conservation may not automatically be guaranteed in numerical methods. The examples of studies related to the momentum conservation in SPH methods can be seen in Bonet and Lok (1999); Khayyer et al., (2009); Khayyer et al (2008) and many others. For the MPS method, Khayyer and Gotoh (2010) studied the momentum conservation property and modified the MPS method to conserve the momentum locally. They showed that due to non-conservation of the momentum equations the pressure evaluated using the meshfree methods has some oscillations. As discussed previously, this oscillations in MLPG_R method are mostly due to non-regular node distribution whilst adopting $\alpha = 0$, i.e. considering only divergence-free form in PPE. In order to overcome the problem, particle shifting technique has to be used, as recently popular in SPH literature (Ye *et al.*, 2019, Lind *et al.*, 2020). The first version of particle shifting (even though it is not named as particle shifting technique) implemented in MLPG_R method (Sriram and Ma, 2012) was based on the minimum pressure gradient. This was very successful in a variety of applications for 2D problems and named as IMLPG_R. However, difficulties are still existing for the 3D problem, particularly near the free surface and near 3D structures, and this will be discussed in the section for future directions.

Recently, Shagun *et al.*, (2021) showed the improved stability in the 3D MLPG_R method by making certain modifications and named the method MLPG_RS. Firstly, the PPE equation was modified by subtracting a linear quantity, $P^* = \rho g (H_0 - z^n)$ from the instantaneous pressure P_{n+1} in Eq. (12+2), where H_0 is chosen as mean still water depth and z is the vertical coordinate. With the assumption of H_0 as constant, P^* satisfies $\nabla^2 P = 0$, and simplifies the boundary condition at walls. This modification allows for a faster convergence for the Poisson equation. The terms in P^* are known from the previous time-step and therefore do not increase the process complexity. In the numerical test cases with identical setup, the Poisson equation solved using bi-conjugate gradient stabilised method achieves convergence in 641 iteration for the original Poisson equation and 194 iterations for the modified Poisson equation. Further, it was pointed out that the earlier derivation (Eqs. (25) to (27)) of integration relied on dividing the sphere into eight divisions and assuming a linear variation of variables within each division for domain integral, and a linear variation along the surface of each division. The resultant expression was asymmetric in space and did not indicate the order of error. Shagun *et al.*, (2021) used Taylor series-based expansion to overcome the disadvantage and then truncate the expression based on an acceptable order of error, i.e. 2nd order. The resultant expressions are symmetric along the 3 axes with a leading error term proportional to R_i^4 (Integration radius, R_i) and require only 6 integration points, simplifying the problem drastically in 3D cases.

Formatted: Font color: Auto

4.2. Governing equations (Single phase) and modelling approach for Wave-Porous/Vegetation Structure Interaction

The governing equation for the porous model is a modified Navier Stokes equation based on Darcy's law, Brinkman's effective viscosity, Forchheimer's linear and non-linear drag force term and Lin's transitional velocity term along with Polubarinova –kochina inertia coefficients, which is given as,

$$\nabla \cdot \vec{u}_D = 0 \quad (28)$$

$$\frac{c_r}{n_w} \frac{D\vec{u}_D}{Dt} = \frac{-1}{\rho_w} \nabla P + \vartheta_{eff} \nabla^2 \vec{u}_D - a \vec{u}_D - b \vec{u}_D |\vec{u}_D| - c \vec{u}_D \sqrt{|\vec{u}_D|} + f_d \vec{u}_D \sqrt{|\vec{u}_D \cdot \vec{u}_D|} + \vec{g} \quad (29)$$

where, C_r is the inertia coefficient; n_w is the porosity, \vec{u}_D is the Darcian velocity of fluid; P is the pressure; v_{eff} is the effective viscosity based on Brinkman (1947); a , b and c is the linear, non-linear drag and transitional coefficients, respectively depends upon the Reynold's number and the type of flow in porous region; f_d is the drag force estimated based on Morrison's equation depending upon square or cylindrical rigid vegetation type (Divya *et al.*, 2020) ρ_w is the apparent density. This is a unified governing equation that can be used for the whole domain with no interface treatment.

$$\vec{u}_D = \frac{1}{v_{tot}} \iiint \vec{u}_f dv \quad (30)$$

$$\vartheta_{eff} = \frac{\vartheta}{n_w} \quad (31)$$

where ν is the kinematic viscosity. These are discussed in detail by Divya and Sriram (2017), along with boundary conditions. If one wishes to adopt for the wave-vegetation interactions, slight modifications of the above equations (removing the coefficient a , b , c) by incorporating inertia and drag forces for square and circular rigid vegetation have been derived by Divya *et al.*, (2020).

The PPE is solved similar to the previous section, which leads to the final general form by including the porous or vegetation region,

$$[K_{IJ}]\{P\} = [F_I] \quad (32)$$

$$K_{IJ} = \left\{ \begin{array}{l} \frac{1}{2\pi R} \int \phi_j(x) ds - \phi_j(x) \quad \text{for Inner fluid particle} \\ \vec{n} \cdot \nabla \phi_j(\vec{x}) \quad \text{for Solid Boundary} \\ \phi_j(x) \quad \text{for free surface particles} \end{array} \right\} \quad (33a)$$

$$F_i = \left\{ \begin{array}{l} \frac{c_r * \rho}{n_v(i) * \Delta t} * \frac{1}{2\pi} \int \vec{u}_D^* d\Omega \quad \text{for Inner fluid Particle} \\ \frac{c_r * \rho}{n_v(i) * \Delta t} \vec{n} \cdot \vec{u}_D^* \quad \text{for solid boundary particle} \\ P_{atm} \quad \text{for free surface particle} \end{array} \right\} \quad (33b)$$

Even though the present weak formulations can handle the discontinuous flow at the interface, the approximation for unknown 'P' are based on Moving Least Square (MLS)/ Simplified Finite Difference Scheme (SFDS, Ma, 2008) interpolation scheme as well as the integrations are based on Gauss quadrature, hence we noticed instability in solving the system of equations due to jump in velocity vectors. To overcome this, the transition interface layer for obtaining porosity (n_w) and resistance terms coefficients (a , b and c) and with smoothing of velocity near to the interface can be employed. The smoothing scheme will be discussed later.

For the wave-porous/vegetation structure interaction, Akbari and Namin (2013) employed ISPH using the background meshes for calculating the porosity, which was initialised throughout the domain. In the MLPG_R, the same idea as that in WCSPH employed by Ren *et al.* (2016) was used, however the transition background nodes are provided only near to this region. In and on other regions the corresponding porosity information are defined. Further, two kinds of particles node distributions are used in MLPG_R. One is the Lagrangian (fluid or porous) particles and the other Eulerian particles (background nodes). The background nodes are finer than the Lagrangian moving particles (fluid or porous). At every time step, the information regarding the drag coefficients and porosity are interpolated from the Eulerian particles to Lagrangian particles. It should be noted that regarding Lagrangian particles only domain integrations and other the calculations on pressure and velocities are carried out. The Eulerian particles will not involve in any computations other than transferring the porous layer information

Many extension and application of Akbari and Namin (2013) approach have been attempted (Akbari and Taherkhani, 2019; Akbari and Pooyarad, 2020). One of the challenging aspects is the imposition of the velocity and stresses in the interface between fluid-porous media. In the ISPH, a numerical smoothing were employed at the interface to improve the stability. On contrary, Khayyer *et al.*, (2018) proposed an enhanced ISPH model with accurate imposition of

velocity and pressure continuity without any numerical smoothing. In the MLPG_R, Zhou and Dong (2018) proposed a sharp interface boundary conditions to couple the fluid-porous medium and provided the successful validations of their model with experimental results. They have extended the two-phase MLPG to this application which will be discussed later.

4.3. Governing equations for rigid floating body dynamics

Newton's second law of motion governs the motion of a floating body. The velocity and acceleration vectors of a floating body are calculated from the following equations

$$[m]\vec{U}_c = \vec{F} + [m]\vec{g}, \quad (34)$$

$$[I]\vec{\dot{\Omega}} + \vec{\Omega} \times [I]\vec{\Omega} = \vec{M}, \quad (35)$$

where $[m]$ and $[I]$ are the mass and inertia matrices, \vec{U}_c is the translational velocity of CG of the floating body, $\vec{\Omega}$ ($\Omega_x, \Omega_y, \Omega_z$) is the angular velocity about the CG of the floating body, \vec{F} and \vec{M} are the hydrodynamic force and moment experienced by the floating body. Once the \vec{F} and \vec{M} are obtained, the accelerations \vec{U}_c and $\vec{\dot{\Omega}}$ can be found out from Eq. (34) and Eq. (35). Then, the velocities \vec{U}_c and $\vec{\Omega}$ are calculated by integrating the accelerations. After the translational velocity and rotational velocity with respect to the CG of the floating body is obtained, the velocity on the free surface of the floating body is updated by using the equation of rigid body dynamics given below:

$$\vec{U}_i = \vec{U}_c + \vec{\Omega} \times (\vec{r}_i - \vec{r}_c) \quad (36)$$

The value of \vec{U}^{n+1} while solving Eq. (24) is unknown. An iterative technique described by Yan and Ma (2007) for fully nonlinear potential flow theory is used in the MLPG_R formulations by Rijas *et al.*, (2019). The algorithm proposed and implemented is given in Fig. 4. In the implementation, the third-order Adams-Bashforth method for predicting the acceleration is employed to decouple the mutual relation between the pressure boundary conditions on the floating body surface and the body acceleration. Theoretically, if the acceleration result is convergent, we can use any scheme for the prediction. The integration of the floating body equations with respect to time needs careful consideration for the overall stability. Numerical tests indicates that the fourth-order Adams-Moulton method were suitable for updating the velocity and position. This leads to convergence in one iteration per time step in most of cases we studied so far.

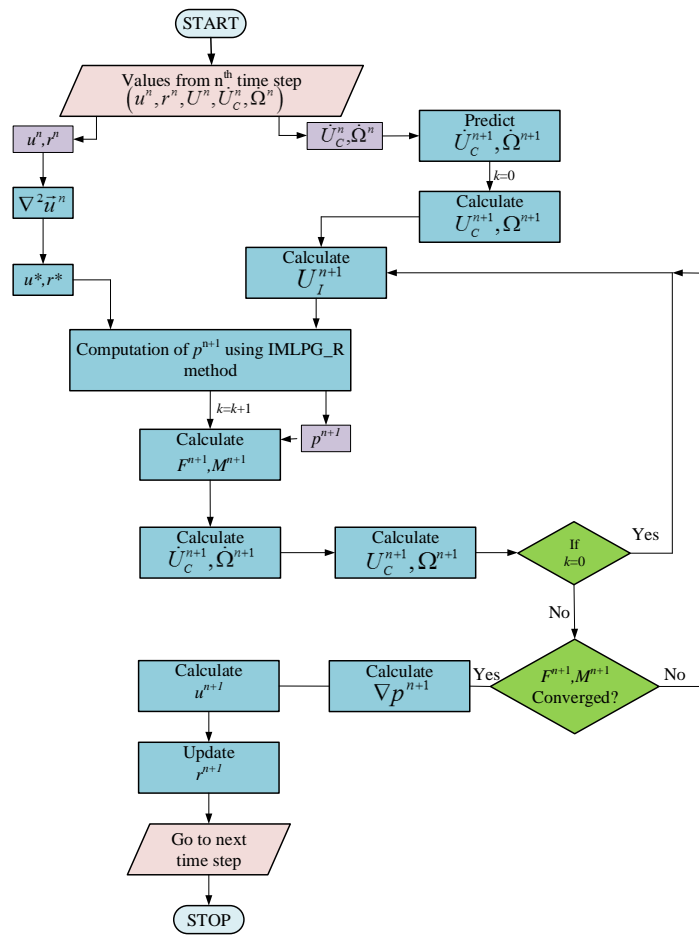


Fig.4. Algorithm for coupling fluid and floating body

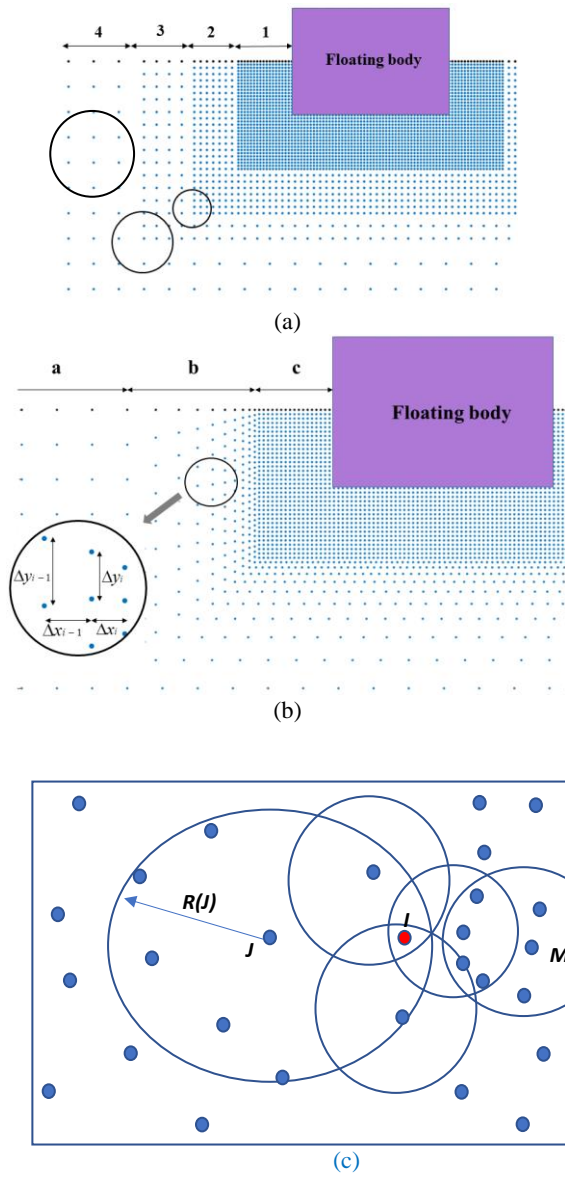


Fig. 5. (a) and (b) Two different variable spacing approach (c) Domain of Dependence and average radius adopted in variable particle resolution.

Further, to accurately capture the flow characteristics of the wave-structure interaction, one needs very fine particle resolution near the structure. Usually, the flow in the domain away from the structure requires only a low particle resolution (i.e., sufficiently capturing free surface waves) compared to the particle resolution near the structure. ~~Suppose uniform particle resolution as fine as that near the structure is used. In that case, the total particle number becomes very high,~~ leading to prohibited computation cost for problems having a large domain. Different resolutions should be applied to different regions, i.e., higher resolution near structure but lower resolution in far-field from the structure to reduce the computation cost without downgrading the accuracy. The variable resolution technique has been widely adopted in mesh-based methods.

Formatted: Font color: Accent 1

In the meshless methods, attempts have also been made to use variable resolutions. However, the specific approach is methodology-dependent. For example, in the SPH method, the variable resolution is achieved by an adaptive way, i.e, starting with a uniform resolution and gradually realising variable resolution by splitting and merging particles (Vacondio *et al.*, 2013). During the process, the SPH equations need to be reformulated. The smoothing length and particle mass associated with it have to be determined based on the distribution of the resolution (e.g., Omidvar *et al.*, 2012, 2013). Due to its nature, it is relatively easier for achieving the variable resolution in the MLPG_R method. That is due to the following factors. (1) The updating of the velocity and position of particles does not involve the mass and volume of particles. (2) The MLPG_R method relies on the SFDI method (Ma, 2008) to estimate the gradient specially developed for random-distributed particles and suitable for variable resolution. (3) The free surface identification schemes discussed in the later section of the paper for the MLPG_R method are also suitable for variable resolution. The only issue for using variable resolution in the MLPG_R method is determining the radius of the support domain (equivalently to smoothing length in the SPH methods); however, it is relatively easy to handle. Due to these features, the MLPG_R method can start with a variable resolution, not necessarily with uniform resolution. Of course, numerical tests need to be carried out to identify the optimum initial spacing of particles. More details about this can be found in Rijas *et al.*, (2019). So far, we have tested two types of initial variable-spacing of particles. One is the sudden change in particle resolution, as shown in ~~Error! Reference source not found.Fig-5a~~ and another is gradually varying of particle resolution, as shown in ~~Error! Reference source not found.Fig-5b~~.

The initial particle distribution like in Fig.5a was used for simulating forced heave oscillation of mono hull and twin hull on the free surface of calm water by Rijas and Sriram (2019). In such problems, the area of interest is the fluid region near the structure, and the radiated waves generated by the body can be allowed to damp out. So, there is no need to care about the outgoing waves for those applications and this stretched nodes in the region away from the body play a role to damp the short waves.

The initial particle distribution like in Fig.5b was employed for simulating the interaction between waves and floating bodies, as shown in Rijas *et al.*, (2019). In this approach, the whole

domain was split into three sub-regions when distributing particles initially: the inner region contacted with the body, the outer region far-away from the body and the transition region. In the inner region, the initial particle spacing should be small enough so that the physics near the structure can correctly be simulated. In contrast, the initial particle spacing in the outer region is determined by the minimum number of particles required for capturing the free surface waves. In ~~Error! Reference source not found.~~Fig. 5b, the initial particle resolution in the inner and outer regions are uniform, but with different spacing. In the transition region, the initial particle spacing gradually decreases from the spacing in the outer region to the spacing in the inner region. The initial particle spacing in the transition region can be determined (e.g. in 2D cases) by

$$\begin{aligned}\Delta x_i &= \gamma \Delta x_{i-1} \\ \Delta y_i &= \gamma \Delta y_{i-1}\end{aligned}\tag{37}$$

where i represents the layer number and γ is the ratio of the particle spacing from finer (inner region) to coarser (outer region). Δx_{i-1} should be greater than or equal to Δx_i . Numerical tests should determine the ratio of the particle spacing γ . The recommended value is 0.6 based on the tests carried out so far. It should be noted that in this approach, the maximum floating body surge should be known before hand in order to define the length-region of the inner region that was in contact with the body. Then, due to the ~~lagrangian~~Lagrangian motion of the particle and enforcing the continuity at the interface, the surrounding particle will move along with the floating body motion.

As indicated above, each particles' radius of the support domain should be determined and treated as dynamic. If one employs constant radius of the support domain for the entire domain, which must be determined according to the particle distance in the region with coarser resolution, it leads to unnecessary large number of particle interaction for finer resolution and overfitting (near the objects). This may lead to increase in computational costs and lead to numerical damping (due to overfitting in the finer resolution region) and increase in computational cost. To overcome this, the weight functions in the MLS/SFDI interpolation scheme was adopted based on the concept of 'Domain of Dependence' (Mukherjee and Mukherjee, 1997). The domain of dependence concept is shown in Fig. 5c. That is, each point has its own support domain with radius $R(J)$ centered at point $x(J)$. The domain of dependence for I is the union of the n overlapping circle (centered at $x(I)$ with radius $R(I)$). For example, in Fig.5c, Pparticle M will not contribute ~~in to~~ the evaluation of I , even though it is nearer than J . Thus n number of nodes in the neighbourhood of an evaluation point ~~with coordinate x~~ for which weight function $W(R_i) \neq 0$ will be considered. However, in order to make sure that I has the same effect on J as that of J on I , the following equation is adopted and proved to option-worked well for the MLPG_R method.

$$R_{IJ} = (R(I) + R(J))/2\tag{38}$$

where I is the particle under consideration and J is the neighbouring particle. The weight function is estimated as $W_{IJ} = W(R_{IJ})$ instead of $W(R_I)$ (Mukherjee and Mukherjee, 1997) for the evaluation point. The radius R for each node is calculated initially based on surrounding particles (average of the 6 nearest node distance in 3D or 3rd node distance with some factor). So, whilst calculating the shape function for regular spaced node, R_{IJ} remains same and support domain will be circular like in standard method. Whereas for irregularly spaced nodes, the radius of the domain or weights for the interaction between I and J particles and J and I particles remain same, ~~however~~ the domain of dependence is non-circular. This is required whilst evaluating the shape functions particularly for the interface nodes as shown in Fig. 5a (marked as 2,3) and 5b (marked as b), ~~where in for other regions where the particles are, such as regularly spaced nodes~~ the domain of dependence becomes circular. At each time step, the radius of the support domain I and J is recalculated based on the neighbours. ~~In order to overcome this issue in SPH for variable particle mass resolution, Omidvar et al., (2013) discussed variable particle mass resolution for SPH and averaged the weights between the particle I and J, however it is not clear whether they have adopted the domain of dependence from their paper.~~

4.4. Interaction between waves and elastic structure

The coupling of the fluid modelling based on the particle method with elastic structure is another challenging task. Two approaches exist, monolithic approach and partitioned approach. The partitioned approach can incorporate any established solvers for the elastic structure, which is also adopted in MLPG_R method. In our investigation so far, we have considered 2D problem, in which the structure is idealised as linear beam using Euler-Bernoulli Equation and solved based on FEM. The two important steps in the partitioned model for solving fluid-structure interaction (FSI) problem are the fluid load transferring from the fluid region to structure and the motion/displacement transferring from the structure to the fluid. These steps ensure that the kinematic and dynamic continuity is satisfied across the domains. The coupling can be strongly or weakly. A weakly coupled method can only ensure kinematic continuity (Wall *et al.*, 2007). In a strongly coupled system, for any region of the wetted (region in contact with the fluid) interface boundary Γ , the dynamic and kinematic boundary conditions can be expressed as Eq. (39) and Eq. (40). Here, σ denotes the stress, and subscripts s and f denote solid and fluid respectively,

$$\sigma_s \cdot \vec{n} = \sigma_f \cdot \vec{n} \quad (39)$$

$$\vec{u}_f = \vec{u}_s \quad (40)$$

In the partitioned approach, kinematic and dynamic continuity requires some special treatments. The method adopted to ensure the continuity of the velocity and normal stresses in the MLPG_R model is based on Farhat *et al.*, (1998). In brief, the interaction is executed in three stages:

(1) Stage 1: estimating the fluid force on the structure. The difficulty to do so arises when the fluid and structure have different spatial resolutions. An interpolation surface may be used to overcome this, as suggested by Farhat *et al.*, (1998). If the spatial resolutions for fluids and structures are the same, the interpolation surface is not required. The fluid pressure can be directly transferred to the structure.

(2) Stage 2: solving the structural dynamics equations. The governing equation for the structure is solved based on the fluid loading estimated in Stage 1. The procedure adopted is detailed in Fig. 5.

(3) Stage 3: Transferring structural kinematic information to fluids. The displacement, velocities and accelerations of the structure are estimated and transferred to the fluid boundary in this stage. Thus, continuity is achieved both in velocity and accelerations (via gradient of pressure in the fluid solver for estimating pressure) and normal stresses.

The two solvers are iterated until the velocities estimated from the fluid and structural solvers achieve the prescribed criteria. During this iterative procedure, the K matrix in Eq. (18) for fluid is theoretically affected by the change in the structural displacement. However, the structural displacement is normally very small in one time step. Based on this, Sriram and Ma (2012) considered the matrix to be constant during the iterations in one step, while F matrix was only updated based on the new velocities. This approach drastically reduced the computational costs based on the tests reported in Sriram and Ma (2012), which was named as near strongly coupled partitioned (NSCP) approach. This procedure is depicted in Fig. 6.

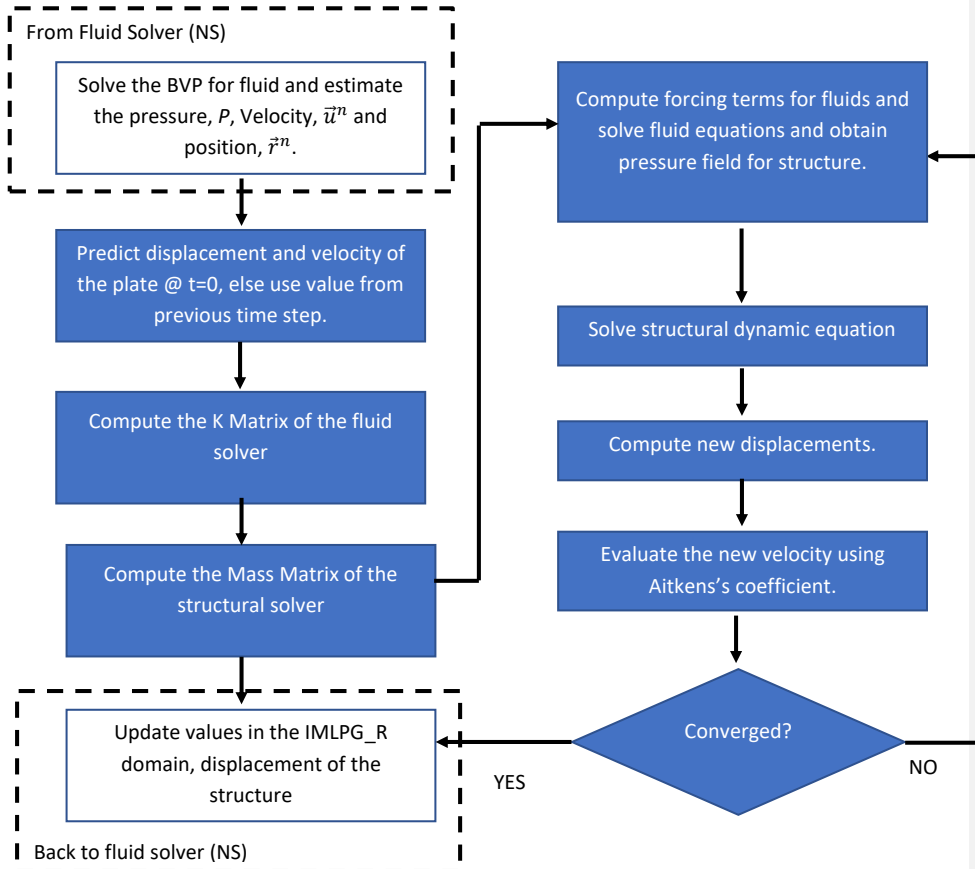


Fig 6: Flowchart depicting the fluid-structure coupling and various stages involved in the process. Different colours show contributions from various subsystems.

In other particle methods, such as in SPH, explicit coupling is mostly adopted. The reason might be due to the small timesteps in SPH, wherein explicit coupling is sufficient. Further, for hydroelastic FSI applications in particle methods two approaches exist. In the first approach, both the fluid and solid domain are discretised using the same particle methods (Rafiee and Thiagarajan, 2009; Khayyer et al., 2018). These are applied to large deformation applications based on Newtonian formulation for structure (like fluids). In the second approach, the particle methods for fluids are coupled with other traditional methods such as Finite Element Method for solids. Attaway et al., (1994) and Johnson, (1994) implemented this approach in SPH. Recently, many authors used SPH and FEM such as Fourey et al., 2017; Long et al., 2017; Zhang and

Wan, 2018). ~~However, in~~In the MLPG_R method, the large deformation problems in wave structure interaction (WSI) have not been attempted so far. However, the MLPG method was quite popular in structure mechanics. Hence the large deformation problem (formulated in Newtonian framework) discretised using MLPG with fluid-structure acceleration approach can be attempted in future work.

Regarding the standard benchmark test cases for WSI, hydrostatic water column with elastic plates is proposed in SPH perspective (See, Fourey et al., 2017). Even though hydrostatic water column with elastic plates is investigated in MLPG (Manojkumar and Sriram, 2020), ~~however~~ the authors ~~felt~~ that the interaction with ~~standing-wave~~ (small amplitude waves) will be more challenging and crucial to ~~know-reveal~~ the performance of ~~the~~ particle method ~~-coupling approach for small amplitude waves~~. The same was investigated ~~by in~~ Sriram and Ma (2012) for the benchmark analytical problem of He et al., (2009).

4.5. Two-Phase modelling in MLPG

Zhou *et al.*, (2017) further developed the MLPG_R method to deal with two-phase flows of fluids with low viscosity and negligible interface tension. When formulating the equations, the two fluids are considered separately. In order to tackle the associated challenges, two new techniques are implemented. The first one is related to coupling the equations for the two fluids, that is the equation for pressure on the interface between different phases. The equation is formed by considering the continuity of the pressure and the discontinuity of the specific pressure gradient (i.e., the ratio of pressure gradient to fluid density). The latter reflects the fact that the normal velocity is continuous across the interface. Zhou *et al.*, (2017) proposed a simple and explicit pressure expression on the interface,

$$p(\vec{r}_0) - \frac{\rho_k \sum_{j=1}^n p_l(\vec{r}_j) \phi_l(r_{j0}) + \rho_l \sum_{q=1}^m p_k(r_q) \phi_k(r_{q0}) - G_r}{\rho_k \sum_{j=1}^n \phi_l(r_{j0}) + \rho_l \sum_{q=1}^m \phi_k(r_{q0})} = 0 \quad (41)$$

The second technique is about solving the algebraic equations for pressure. A newly formulated pressure equation achieves the coupling between two phases for interface particles (Eq. (41), which forms the algebraic equations for pressure together with discretised Poisson's equation at inner and rigid wall particles (Eq. 16). To solve the algebraic equations, two approaches are proposed and investigated. One approach (Integrated-1 Approach) is to solve the pressure equations for different fluids as one system, while the other (Coupled-2 Approach) is to split the whole set equation into two coupled sets and find the solution by iteration between the two sets. The results showed that both approaches can work well for the cases with low density ratios, where the Coupled-2 Approach is more computationally efficient. When the density ratio is high, only Coupled-2 Approach leads to correct results.

Further, to implement the interface condition, the interface particles need to be explicitly identified, especially for large deformations or free surface breakings. The technique based on absolute density gradient (ADG) developed in Zhou and Ma (2018) can be adopted with the criterion of $0.3 < \beta/\beta_0 < 1.5$ for interface particles, where $\beta = |\rho_x| + |\rho_y|$, $\beta_0 = |\rho_k - \rho_l|/\Delta l$, with ρ_x and ρ_y being the density derivatives in horizontal and vertical directions respectively, and Δl is the initial particle distance. If the ratio is less than 0.3, the particles are justified as inner particles while those with the ratio larger than 1.5 are judged as isolated particles. The tests have also been carried out for different values near the upper boundary, i.e., from 1.4 to 1.6. More details of the technique for identifying the interface particles can be found in Zhou and Ma (2018).

It should be noted that although the three techniques discussed above are developed in the framework of MLPG_R method, the concepts may directly be implemented by other particle methods, including ISPH and MPS.

The two phase modelling in SPH and MPS has been carried out by many authors ~~for various different problems, and improved advancements are proposed in modelling the problems~~ such as air-water interactions (Colagrossi and Landrini, 2003; Dao, 2010; Fonty et al., 2020), ~~c-~~ Compressible air- incompressible water (Luo et al., 2016; Lind et al., 2016); classical bubble rising study (Grenier et al., 2013; Zhang et al., 2015); boiling generated bubbles and dynamics using MPS-SPH (Duan et al., 2020); oil spill studies under the wave actions (Shi et al., 2018; Shimizu et al., 2020); wave impacts on the structure (Lind et al., 2015; Rafiee et al. 2015; Sun et al. 2019); water entry ~~problems~~ (Yan et al., 2015; Khayyer and Gotoh, 2016; Yang et al., 2020), ~~and so on.~~ All the above studies proposed improved algorithms ~~in-for~~ coupling two different methods/solvers or same methods ~~but~~ with or without compressibility. ~~Benchmark problems shows promising improvements.~~ Nevertheless, real applications with turbulence; in-depth analysis on the dynamic response of the air-pockets and its influence on the cushioning effect in reducing the pressures; the relationship between impact pressure and air-pockets, and so on, need to be investigated further. ~~It should be noted that scale effects plays a major role, the tests that were conducted in small scales will not have compressibility effect when compared to large scale studies. So under such circumstances, use of compressible model for air phase should be considered seriously. For example, in breaking wave impact with vertical wall, the large scale studies will lead to large forces and pressures than small scales. However, when one uses the Froude method to upscale the small scale results, it will lead to larger forces and impact pressures than large scale. This indicates that compressibility of air is negligible in small scale (See, Ravindar et al., 2022 for detailed discussion and proof from experiments on this topic).~~

Commented [MQ1]: It does not have added values to discuss scale effects here.

4.6. Other Numerical techniques:

4.6.0. New interpolation schemes

To more consistently and efficiently estimate pressure and its gradient in MLPG_R method, a new interpolation scheme named as Simplified Finite Difference Scheme (SFDI) was introduced by Ma (2008). The numerical test showed that the SFDI was suitable for random particle distribution and can achieve the same or better results as the moving least square (MLS) method but using less computational time. The SFDI can work under situation of small number of neighbour particles where MLS method fails. Recently, this method was redeveloped into QSFDI by Yan *et al.*, (2020) by involving high order terms. The new formulation can also be employed for estimating Laplacian of a function. This opens a new way to approximate the Poisson's equations. The SFDI has also been adopted in some publications based on the SPH method to solve different problems, including breaking wave interaction with fixed cylinder (Zhang *et al.*, 2021), flexures of ice floe (Zhang *et al.*, 2019a) and ice-ship interactions (Zhang *et al.*, 2019b), which shew that SFDI can improve the accuracy in estimating gradients and derivatives.

4.6.1. Scheme for velocity smoothing

Normally, smoothing of velocity will be carried out in particle methods to reduce the instability issues. For example, Ma (2005a) proposed the following formula to smooth the velocities in MLPG and subsequently adopted in various applications using MLPG:

$$\vec{u}_i^n = (1 - \gamma_v)\vec{u}_i^n + \gamma_v \sum_{j=1}^N \phi_j \vec{u}_j^n \quad (42a)$$

where ϕ_j is the shape function ~~arrived~~derived from MLS and γ_v normally taken as 0.15. This is similar to XSPH proposed by Monaghan (1994):

$$\frac{d\vec{r}_a}{dt} = \vec{V}_a + \varepsilon \sum_b m_b \frac{V_b - V_a}{\rho_{ab}} W_{ab} \quad (42b)$$

For clarity, the same notations that was employed in SPH has been used in the above equations. \vec{V}_a corresponds to the velocity \vec{u}_i^n , b corresponds to number of neighbours like j in Eqn. (42a).

$\varepsilon = 0.5$ in XSPH. If one assumes mass and density as constant (incompressible MLPG) and consider MLS shape functions as weight function, then after rearranging the terms, Eqn. 42b can be rewritten in the form of Eqn. 42a. Thus, in XSPH the smoothing scheme employed is similar to MLPG, though the coefficient is larger compared to MLPG.

4.6.2. Free surface identification methods

It is essential to identify the boundaries properly and assign the boundary values to obtain a stable solution. Particularly when modelling the problems involving breaking waves in single phase flow, one needs to identify the free surface particles on which the Dirichlet boundary conditions should be applied, i.e., $p = 0$. In the MLPG_R domain, the particles used for simulation falls in three categories

1. The particles that make up the free surface.
2. The particles that form other boundaries (rigid/flexible walls, bottom boundary, structure surfaces, etc.).
3. The interior particles.

Identifying the free surface particles is challenging as they will be kept changing in breaking waves, i.e., the particle on the free surface may become interior particles. Some time, interior particles may emerge as free surface particles. Several different approaches for identifying free surface particles have been developed in MLPG_R method. Three approaches will be discussed briefly.

4.6.2.1. Mixed Particle number and Auxiliary function Method (MPAM)

Ma and Zhou (2009) and Zhou (2010) proposed Mixed Particle Number and Auxiliary Function Method (MPAM) to identify the free particles for modelling breaking waves. This method was introduced to overcome the Particle Number Density (PND) Method proposed by Koshizuka and Oka, (1996) for the MPS method. The following equation calculates the particle number density (n_i) at a particle I

$$n_i = \sum_{j=1, j \neq i}^M w(|\vec{r}_j - \vec{r}_i|), \quad (43)$$

where M is the total number of particles within the support domain of Particle I , and w is the weight function. The free surface particles are identified if the parameter $\beta_i = \frac{n_i}{n^0}$ is smaller than a value, where n^0 is the initial value of the PND. Ma and Zhou (2009) observed that this method may fail during wave breaking and when particles get close to each other during the simulation. To improve the state of the PND method, Ma and Zhou, (2009) used three auxiliary functions ($aux_{fun1}(I)$, $aux_{fun2}(I)$, $aux_{fun3}(I)$) in each quadrant of the support domain and combined them with PND method to form the MPAM. This method considerably reduce the misidentification and improve the results. A detailed explanation of the method can be found in Ma and Zhou (2009) and Zhou (2010).

4.6.2.2. Combination of Scan cone and MPAM method

In the MPAM, the particle number density is essential, and it needs to be estimated at each time-step. The particle number density requires that the initial node distribution be equally spaced. Employing the MPAM alone may overcome this disadvantage. However, it is time consuming due to search in every quadrant. [The method suggested by Bascasco *et al.*, \(2013\) was adopted in the MLPG_R method instead of PND to overcome this issue. Even though this method was used along with the SPH formulation in that reference, the approach is purely geometric and independent of the SPH formulation. Hence, this technique can be directly incorporated along](#)

with any Lagrangian methods including the MLPG_R method. This method is based on the intersection of circles. Initially, the cover vector \vec{b} is defined as:

$$\vec{b}_i = \sum_{j=1}^{N_i} \frac{(\vec{r}_i - \vec{r}_j)}{|\vec{r}_i - \vec{r}_j|} \quad (4244a)$$

Based on this cover vector, Barecasco *et al.*, (2013), proposed the scan cone searching for every particle as,

$$\arccos \left(\frac{(\vec{r}_i - \vec{r}_j) \cdot \vec{b}_i}{|\vec{r}_i - \vec{r}_j| |\vec{b}_i|} \right) \leq \gamma \quad (4344b)$$

If one particle satisfies the above relation, then that fluid particle is considered a free surface particle. In the present study, the value of $\gamma = 0.523$ was chosen based on our numerical test. When this technique was used in MLPG_R, there were issues identifying the free surface particles when the wave face was nearly vertical. To overcome this difficulty, the Auxiliary functions from MPAM was used along with the scan code method. A flow chart of the scan cone method and MPAM used for free surface identification implementation is given in Fig Fig-7. To speed up the searching process, an initial sweep is being carried out. For this, the magnitude of gradient of the position vector (\vec{r}) is estimated (α_N). Based on our numerical test, the value greater than 0.3 is considered as a free surface. This reduces the searching region for the free surface particle. Thus, the combination of three above schemes reduces false positive, while looking for free surface particles, as shown in Fig. 7. This approach is particularly suitable for cases involving physical phenomena such as wave overtopping on coastal structures and green water loading on decks and whilst employing variable spaced particle in MLPG.

4.6.2.3. Simple Free surface identification in 3D

For a non-breaking wave without any 3D structure, there is no requirement of any special approach to identify the free surface particles. However, with the 3D structure present in the flow, due to the wake and interactions near the 3D structure, some of the free surface particles will penetrate and some of the inner particles will emerge near the free surface locations. Hence, these needs to be detected properly to estimate the pressure accurately. Shagun *et al.*, (2021) during his implementation in 3D domain, proposed a simple free surface identification scheme instead of the two-step algorithm as discussed above. For a node I , a summated unit displacement vector is calculated as shown in Eq. (44).

This equation is considered for $|\vec{r}_i - \vec{r}_j| \leq R_f$. Here R_f is a size of a spherical sub-domain around node i , calculated using M closest neighbours given by

$$R_f = \frac{\beta}{M} \sum_{j=1}^n |\vec{r}_i - \vec{r}_j| \quad (4445)$$

In the preliminary work for the application on wave-cylinder interactions, $M = 6$, $\beta = 2.0$ and $\alpha_N = 0.24$ were used (See Fig.7; Reduces the number of particles that needs to be considered). It

Formatted: Font: Times New Roman, 12 pt, Font color: Text 1

was shown that this approach alone however will identify nodes near corners and faces of the domain as free-surface. Nevertheless, to be successful in this approach, one need to add a single layer of ghost nodes along the outward normal of the side, bottom and body faces, placed at a distance of $0.55R_f$. In case of highly irregular node distribution, two or more layers of ghost nodes along the outward normal can be used. This approach eliminates the misidentification problem for the free-surface nodes near the structure due to the disturbance. However, this approach was not yet tested for the incoming breaking wave problems. In those cases, the subsequent two algorithms, scan cone and MPAM might be required, which needs to be investigated further for 3D.

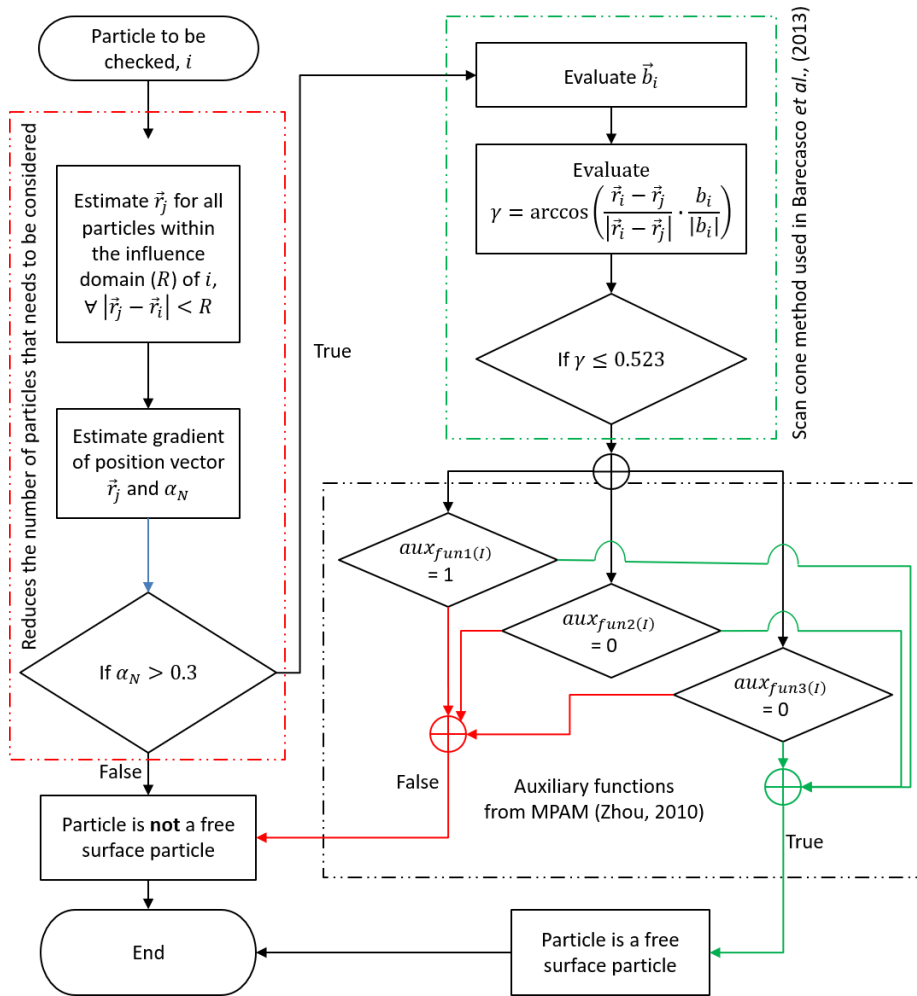


Fig 7: Scan cone method and MPAM for identification of free surface particles. For Auxiliary functions definitions refer Zhou (2010).

4.6.3. One-way and Two-way coupling with FNPT

In ocean engineering applications one needs to model the large scale – both in space (ranging from km² to m²) and time (hours to sec). There are two grand challenges for numerical

modelling based on the NS theory for this kind of problems. One is that simulating wave propagation in a large domain and long duration will inevitably suffer from numerical damping, irrespective of the methods (mesh and meshless), i.e., some of wave energy dissipated by the numerical damping. Another is that such NS models take too long time to yield desired results which is a hindrance for practical/industrial use. On the other hand, the FNPT models are more computationally efficient and does not suffer significant numerical damping. However, they are inheritably unable to consider the viscous effects and to deal with breaking waves and their interaction with structures. The teams led by the authors of the paper have started to develop hybrid methods coupling the NS and FNPT models since 2010. Usually, in the region near structure or with potential breaking waves of interest, the NS model is used whilst the FNPT model is employed in the far field if the domain partitioning approach is adopted. They explored different coupling strategies, including the mesh-based (Li *et al.*, 2018; Gong *et al.*, 2020) and meshless methods (Sriram *et al.*, 2014; Zhang *et al.*, 2021; Shagun *et al.*, 2021) for NS model. Below, a summary on the coupling of meshless MLPG_R method with the FNPT model will be given.

There are two kinds of coupling: one-way (weak) and two-way (strong) coupling. In one-way coupling, only the information from FNPT model is transferred to the NS model while in the two way coupling the information from the two models are mutually exchanged. Fig. 8 shows the basic concept of the coupling for the MLPG_R method with a FNPT model.

4.6.3.1. One-way coupling

The one-way coupling can be regarded as a way that the FNTP model generates waves for the MLPG_R domain. The one-way coupling between a FNPT model (Sriram *et al.*, 2006) and 3D MLPG_R method was reported by Shagun *et al.*, (2021). The moving overlapping strategy, as shown in Fig. 8d, is used for this approach. Its procedure is described below.

Step 1: Run the FNPT model for whole domain and extract the velocity, pressure and free surface elevation in a region at the coupling interface or overlapping zone for the entire duration of the simulations.

Step 2: Interpolate the variables in the MLPG_R domain at a required particle position surrounding FNPT nodes to estimate the pressure and velocity.

Step 3: The extracted values of pressure are applied at the boundary of MLPG_R domain at required locations/area.

Step 4: After solving the MLPG model, there will be reflection from the structure towards the generating or initial region. This needs to be suppressed for long time simulations. The estimated velocity from MLPG and the velocity from FNPT will be similar (as they have simulated without any structure). In order to achieve this, the following correction is made.

$$\bar{u}_p = (1 - \alpha) \bar{u}_{FEM} + \alpha \bar{u}_{MLPG_R} \quad (4546)$$

where α is given by $\alpha = 1 - 3\left(\frac{x-x_l}{L_c}\right)^2 + 2\left(\frac{x-x_l}{L_c}\right)^3$

x_l is the left most location at zeroth time step and L_c is the length of the coupling region. Apart from matching the velocity, it is also required to ensure the continuity of the free surface elevation to have a smooth varying profile.

In the above procedure, the coupling is mainly carried out using Dirichlet boundary conditions. However, some publications for the SPH method use Neumann boundary conditions, i.e. it provides velocity at the inlet boundary conditions. This is the marked contrast with the approach in the MLPG_R method. Mathematically, whilst solving PPE, it is better to specify the known pressure at the boundary instead of the velocity (i.e Neumann boundary conditions). One way coupling in SPH with shallow water equation or by Boussinesq equations ~~are have~~ also been investigated (notable works are Narayanaswamy et al., 2010; Kassiotis et al., 2011; Altomare et al., 2015; Ni et al., 2020). Fourtakas et al., (2018a) adopted one way coupling between ISPH and a FNPT solver QALE-FEM (Ma and Yan, 2006) following the procedure outlined in Sriram et al., (2014).

4.6.3.2. Two-way coupling

In the above approach on one-way coupling, the potential flow model will be simulated without feedback from the NS model for all time steps. Whereas, in the two-way coupled model, the information from the NS model is also feedback to the potential model. Thus, the coupling has to be implemented both in space and time. For coupling in space, Sriram *et al.*, (2014) proposed four different options based on Eulerian and Lagrangian approaches. This is illustrated in Fig. 8 with some updates based on the authors recent experiences. Among the options, we found the overlapping zone approach was better than the others, i.e., the options (c) and (d) are superior irrespective of Eulerian or Lagrangian models.

In the particle-based method, we have mostly employed moving overlapping zone method as shown in ~~Fig Fig-9~~. The figure snapshot is taken from the actual simulation to explain the procedure. In our approach, the coupling boundaries are allowed to move. The line B_2 denotes the boundary for the FNPT domain and always moves along with the free surface and is kept straight (adopting quasi-Eulerian and Lagrangian approach). The line B_1 represents the boundary for the NS domain, and it can change in its shape (based on wave kinematics). Here, L_f and L_o are lengths of the fluid domain of the FNPT model and the overlapping zone respectively at the time t^n (Say, $t = 4.5s$, wherein the waves haven't propagated into the NS domain) . As the simulation advances to the time t^{n+1} (Say, $t = 12.5s$, wherein the waves have propagated into the NS domain), the lengths of each zone changes to $L_f + dL$ and $L_o + dS$. As can be seen, there are three boundaries. In addition to B_1 and B_2 , there is also the boundary B_0 . The particles in the region between B_0 and B_1 (called as feeding particles) participate during the interpolation in the

Formatted: Font: Times New Roman, 12 pt, Font color: Text
1

MLPG_R model and the pressure and velocity at them are calculated by the FNPT model. The algorithm for the two-way coupling is further illustrated in Fig. 10 and discussed below.

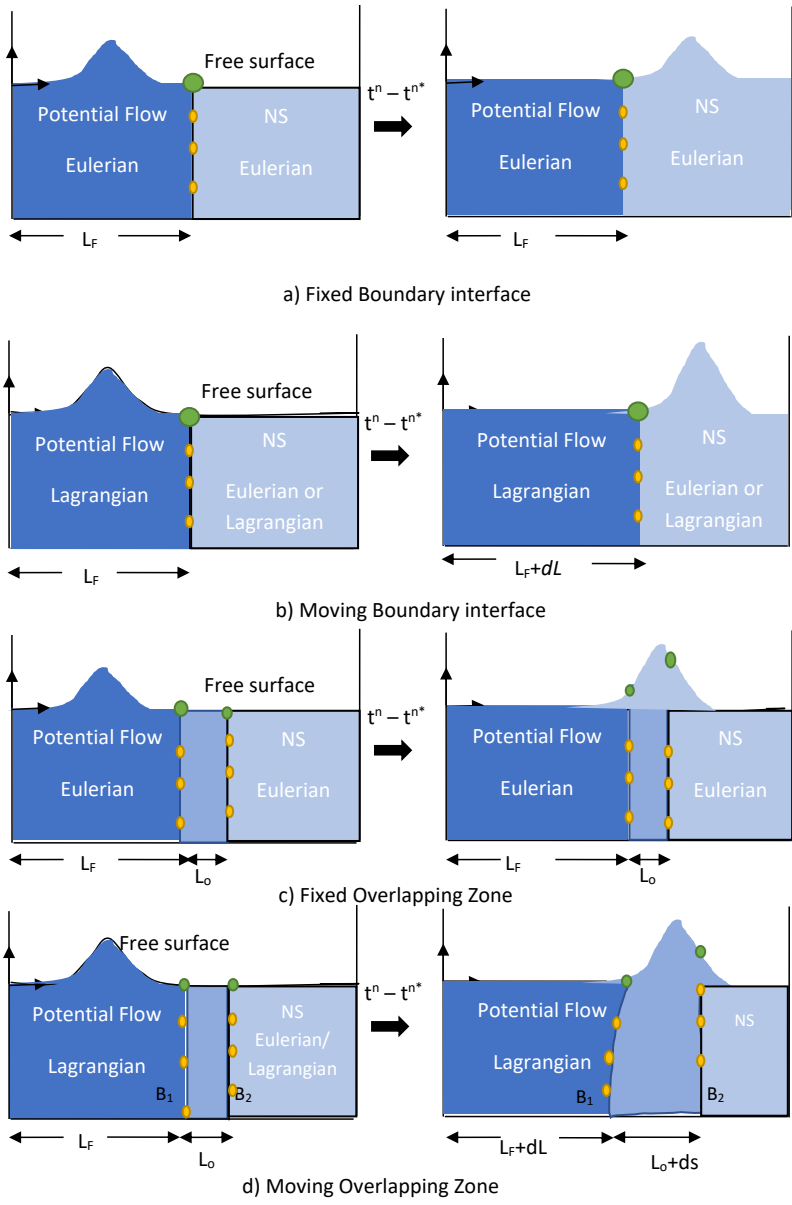


Fig.8. Different space coupling approaches (yellow– velocity or pressure boundary; Green– Free surface boundary condition). Reproduced and updated from Sriram *et al.*, (2014)

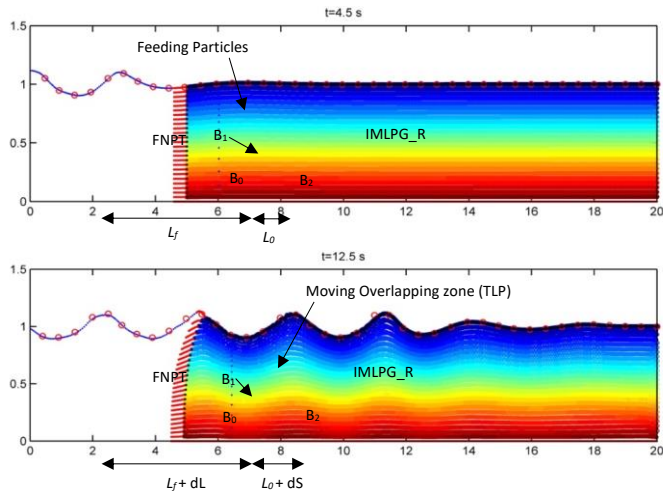


Fig 9: Concept of moving overlapping zone from Sriram et al. (2014) for simulations of regular waves. TLP Stands for Two Layer Particle, wherein FNPT and NS will be solved.

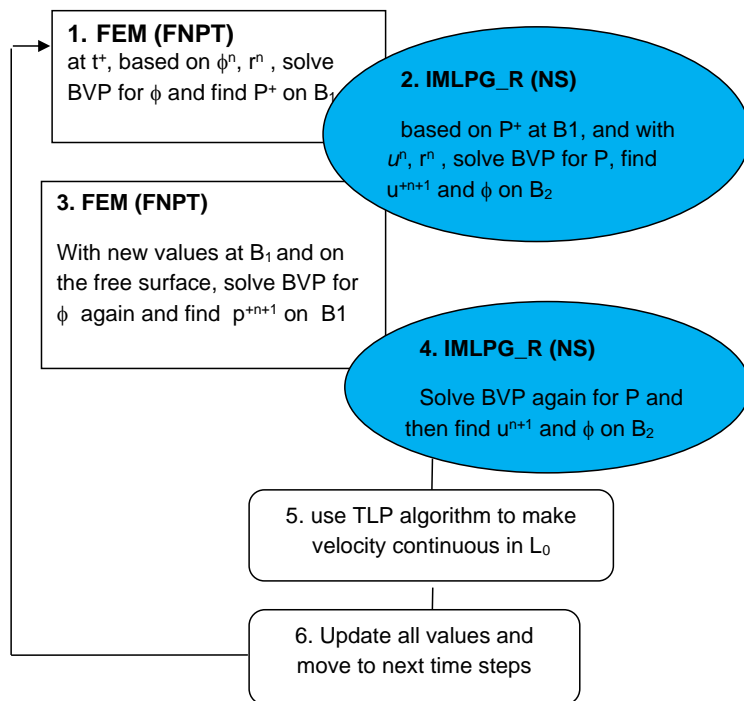


Fig 10: The algorithm showing the two-way coupling process between the MLPG_R and FNPT models; ϕ is the velocity potential. r is the position of the particle at an instant. p^+ is the intermediate pressure. n and $n + 1$ denoting the current and future time steps.

The algorithm starts from the time step $t = t^n$, where all the variables, such as velocity (u), velocity potential (ϕ), position (r) and pressure (p) are known. The intermediate value of velocity potential, the intermediate value of pressure, $p = p^+$ on the boundary B_1 is estimated by solving the boundary value problem for ϕ . B_1 depicts the boundary of the MLPG domain. Based on the boundary values of pressures obtained from the simulations carried out in the FNPT, the

boundary value problem for pressure was solved in the NS domain. The boundary value on the FNPT domain is updated based on the estimates from the NS. (See, Fig.10).

Another critical factor to be kept in mind here is that we have two different solvers using two different time integration approaches. The FEM uses explicit 2nd order or 4th order Runge–Kutta time integration while the MLPG_R uses explicit Euler time integration. So, for coupling both the models, a predictor-corrector approach as shown in Fig. 10 is employed.

Similar to one way coupling, ~~mostly in two way coupling~~ the fixed overlapping zone ~~can be~~ applied ~~in two way coupling~~. However, an interesting work attempted in MPS ~~needs~~ to be pointed ~~out~~. Sueyoshi et al. (2007) proposed the MPS method at the top part of the domain near the free surface while the bottom part of the domain was modelled by using the BEM. The information between the two solvers were transferred through a fixed boundary interface based on the Neumann type boundary conditions. Verbrugge et al., (2018) proposed a two way coupling between OceanWave3D and DualSPHysics. The model was validated for propagation of linear and nonlinear waves along with a typical application of oscillating water column and 2D floating body simulations. The issues ~~with~~ oscillations was noticed and it was attributed to the WCSPH as well as implementation of dynamic boundary conditions related to the fixed boundary interface. The issues associated with fixed overlapping boundaries have ~~already~~ been pointed ~~out~~ in the previous sections. This was initially tried in the MLPG_R method and was not successful, hence Sriram et al., (2014) proposed a moving overlapping with pressure as an input whilst solving PPE in 2D. The same approach was also successful in our 3D approach (Agarwal et al., 2020).

Manoj Kumar and Sriram (2021) extended the elastic structure interactions in MLPG_R, by considering three domains, a inviscid fluid domain (FNPT) solved using FEM, a viscous fluid domain (NS) solving using MLPG_R and a structural domain solved using FEM. In the hybrid coupling approach discussed in Fig. 10, a predictor-corrector scheme has been employed. Hence, the elastic structure equation can be solved in every stages or selected stages within an time step whilst solving the NS domain. The physical reason for this is that the structural deformation needs to be accounted in the viscous fluid domain and vice versa. Since the time-step at which the model operates is so small (normally, $\Delta t \leq 0.0015$ s for the FSI problems), the differences in plugging the structural solver at different model stages should not affect the results. However, Manoj Kumar and Sriram (2021) carried out a rigorous testing during the validation phase and showed some deviation among the implementations. The authors investigated three possibilities as listed below to show its influence,

1. Solve the structure equations only in the predictor step in MLPG. In the predictor step, Fig. 5 scheme will be applied. (Algorithm A).
2. Solve the structure equations only in the corrector step but, use the previous results for the predictor step. (Algorithm B).
3. Solve the structure equations for both predictor and corrector steps. (Algorithm C).

The difference between these algorithms lies in the quality of pressure forcing obtained at the fluid-structure interface. In Algorithm A, the pressure on the structure is based on the first intermediate pressure obtained after solving the BVP for pressure in the NS domain. During the corrector stage, FSI is not invoked. In Algorithm B, the fluid forcing on the boundary is estimated based on the corrected pressure at the final step. Thus, FSI makes use of the corrected pressure to calculate structure displacement and velocities. In this case, the FSI is not invoked in the predictor stages. In third approach, FSI is invoked during both predictor and corrector stages. This is called as Algorithm C. Again in Algorithm C, there are two possibilities whether to initiate A and B or B and A. Thus, the procedure is going to depends upon the numerical schemes and the implementation strategies. The authors finally concluded that the difference is due to the numerical estimates at the first-time step, while executing algorithm A (small numerical difference in pressure and velocity estimates) by comparison with analytical solution for hydrostatic test. Finally, they concluded that Algorithm B and Algorithm C (in the order of executing B & A) produces identical results and good comparison with the analytical solution. Further, the computational time (total time required for simulation) in all these algorithms were also similar.

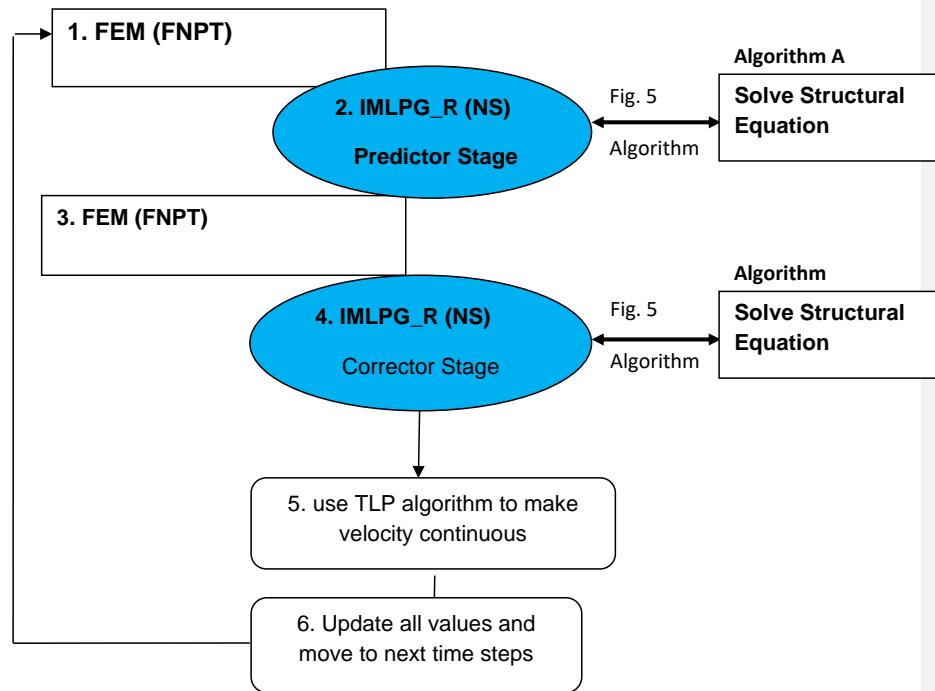


Fig 11: The algorithm for coupling MLPG_R and FNPT models to deal with fluid elastic structure interactions.

5.0. Applications modelled by the MLPG_R method

In this section, applications of the MLPG_R method are briefly discussed for dealing with various types of waves and their interaction with structures. [Details regarding the SPH applications were reviewed recently by Luo et al., \(2021\)](#). For ocean engineering applications, a numerical tool should have the following features.

- (a) Simulate small and steep (non-breaking) waves accurately;
- (b) Model plunging/splash-up (breaking or violent) waves rigorously;
- (c) Handle the interactions of complex violent waves with rigid and/or elastic structures robustly.
- (d) Have high efficiency in simulating such cases.

Our developments in MLPG are specifically tried to achieve these features. Fig. 12 shows a typical comparison between the analytical free surface profiles (both in space and time) with

MLPG_R methods. The total number of nodes used is 16000 with a timestep of 0.01s for this simulation. Similarly, the results of the 3D MLPG_RS method for uni-directional focusing waves compared with that of potential flow theory are provided in Fig. 13, showing the capturing of all free harmonics, super and sub harmonics components in the free surface elevation. The interaction of the uni-directional focusing waves with the cylinder is shown in Fig. 14. One interesting aspect is how well the present MLPG_RS method compares with the other particle methods, such as SPH. One such comparison was recently reported in Sriram *et al.*, (2021) as part of the comparative study carried out in ISOPE. The results are reproduced in Fig. 15 for an identical case between 3D MLPG_RS and SPH. It can be seen that the MLPG_RS methods shows good agreement with experiments without any artificial fluctuations which can be seen in the results of SPH method for this case. Further, the 2D IMLPG_R method has been applied to modelling wave-porous structure interactions and wave-vegetation interactions in recent years. One typical example of solitary waves propagating over the vegetation region is shown in Fig. 16. The proposed model was validated with the existing numerical, analytical and experimental work for regular wave and solitary wave interaction with the vegetation. The details are reported in in Divya *et al.*, (2020). The porous wave structure interaction was detailed in Divya and Sriram, (2017).

Apart from modelling the small and steep waves with ease, MLPG has also been applied to breaking waves interactions or overtopping applications. Typical snapshot of the overtopping over different types of coastal structure is shown in Fig. 17. One can notice there is no spatial oscillations in the velocity magnitude. The model was also applied to long distance wave propagations and undular breaking bore on the slope. A typical application using the coupled hybrid model is shown in Fig. 18, where a runup of thin layers from elongated waves are modelled with ease. However, turbulence and boundary layers are not resolved in this application, which should be attempted in future. The wave breaking interaction with a 3D structure is shown in Fig. 19. One could see the velocity magnitude on the free surface and pressure just above MWL are free from any numerical oscillation unlike other particle methods, which lays good foundation for modelling interactions between floating body and elastic structures with breaking waves, as the artificial oscillation can leads to instability or fail the modelling process during such interactions.

A typical application of the 2D IMLPG_R method to model a floating body using variable particle spacing is provided in Fig. 20. From the figures, one can see that the method well handles the large displacement of the floating body with higher resolution region following the body movements. The adaptation of the neighbouring particles along with the floating body motion for large displacement can be seen. This is possible due to the different schemes such as ensuring continuity between the fluid and floating body velocities, smooth pressure and pressure gradient estimation and avoiding any clustered node distribution during simulation as discussed in the numerical treatment sections. Fig. 21 shows another case with the green water effects happening on the top of a floating section.

Modelling complex wave breaking with elastic structure was attempted by Sriram and Ma (2012). Fig. 22 shows the comparison of the experimental high-speed images with MLPG_R method. There are slight leakage through the elastic plate in the experiments, as can be seen in the second or third row of the figure (as well as personal communication from Dr. Oliver

Kimmoun). As the numerical model is two-dimensional, no such leakage exists, which leads to some difference in the return profile as depicted in the figure. Nevertheless, the method predicts a small wave overturning and the deflection of plate compared to experiments (See, Sriram and Ma, 2012 for details), which is challenging in the particle method. For such a case, a large number of particles are normally required in other class of particle methods otherwise it will be difficult to correctly capture the overturning. In addition, it also requires more iterations to converge within a time step compared with modelling a problem for a rigid body. Hence, to reduce the computational time, a coupled model formed by combining a FNPT at the far end with NS model near the structure was proposed by Sriram *et al.*, (2014) as described early. They demonstrated that the hybrid method needed only one-eighth of a NS model to achieve similar results, though the saving may be problem-dependent. The technique proposed by Sriram *et al.*, (2014) is adopted subsequently in other methods with some improvements, such as in qaleFEM-SPH, qaleFOAM and so on (See, Sriram *et al.*, 2021). By adopting this hybrid coupling, Manoj Kumar and Sriram (2020) studied regular wave interactions with elastic plate. Further, Manoj Kumar (2021) studied the focusing wave interaction with the horizontal elastic plate as shown in Fig. 23, wherein a comparison of the experimental snapshot is also provided. The figure demonstrates that the numerical model well captures the physical phenomena observed in experiments, i.e., after the focusing wave impacts near the corner, the flexible plate deflects downwards (or starts to vibrates), which in turn interacts with the incoming waves creating a slamming effects.

The hybrid method does not only save the computational time but also reduce the numerical dissipation suffered by NS solvers for modelling long distance and long duration propagation of waves. This was also pointed out by Grilli (2008) and Sitanggang, (2008). Based on our experience the numerical dissipation will occur approximately after 15L and 20T (L and T corresponds to wave length and period). To demonstrate this, wave propagation in a tank length of 100m with a water depth of 1m is simulated by using the MLPG R method without considering physical viscosity. Two different wave parameters are considered, one with a smaller amplitude and the other with a larger amplitude waves ($H = 0.14$ and 0.26 , corresponding to wave steepness $H/L = 0.0216$ and 0.0499 , respectively). The wave elevations reading at two different locations together with the FFT results of the elevation are shown in Fig. 24. One can see that from this figure, the smaller amplitude waves (Fig. 24b) have much less numerical dissipation compared to the larger amplitude waves (Fig.24d). The latter shows about 6% reduction with respect to FNPT results. One can also see the larger phase shift in the wave elevation for the steeper wave. This occurs due to reduction in the wave height leading to the reduction of the wave celerity. The numerical dissipation is expected to be decreased by increasing the resolution of particles, but this requires higher computational costs. The better way is to employ a hybrid method discussed above. It can be deduced that if the cases would be run by using a hybrid method, the numerical dissipation would be insignificant as already seen in Fig. 13.

Formatted: Font color: Light Blue

Formatted: Font color: Accent 1

Formatted: Font color: Accent 1

Commented [MQ2]: I am not sure what method you used, Please confirm and change accordingly.

The application in modelling multiphase flows is another milestone of MLPG_R method development. For both real natural environment and engineering practice, the density ratio of different fluids involved can approach 1, such as stratified fluid flows in oceans, or reach more than 1000, such as the water-air flows. The modelling robustly for the problems with lower and high density ratios is challenging for many numerical methods. Zhou *et al.*, (2015) developed the scheme in the MLPG_R method, which was not only robust for small density ratio, but also high density ratio more than 1000. Fig. 24-25 shows the pressure distribution in a tank with sloshing liquids, depicting a smooth variations at the interface. Later, the same approach was extended to wave-porous structure interaction in Zhou and Dong (2018).

Formatted: Font color: Accent 1

~~Finally, the fourth point efficiency in simulation has been addressed in some of our papers. There are many ways to reduce the computational aspects (a) using the parallel computing, GPUs, OpenMP based on high performance computing (c) physics based approximations. In our development, before venturing into first approach, we implemented the second approach that is physics based approximations. This was discussed earlier, however it should be noted that the increase in computational time is a secondary effect. The computational aspect of the MLPG in 3D for the problem of wave fixed cylinder interactions with that of other class of particle and Mesh based solver from 20 different solver is reported in Sriram *et al.*, (2021), showing better than other class of particle method. The main purpose of implementing the physics based hybrid approach is that NS solver exhibit numerical dissipation for long distance propagation. This was also pointed out by Grilli (2008) and Sitanggang, (2008) when they coupled with the mesh based NS solvers. Based on our experience the numerical dissipation will occur approximately after 15L and 20T (L and T corresponds to wave length and period). However, to show the numerical dissipation characteristics, a tank length of 100m with a water depth of 1m is considered. Two different wave characteristics one with small amplitude and other with steep amplitude waves were generated ($H = 0.14$ and 0.26), corresponding to wave steepness ($H/L = 0.0216$ and 0.0499 respectively). The wave probe reading at two different locations are shown in Fig. 25. More importantly, from the time history, the phase shift was observed at the larger distance. This is occurred due to reduction in wave height changing the celerity. Further, this is more pronounced for steep waves. To show the numerical dissipation, representing in frequency domain the small amplitude waves, (based on FFT, Fig. 25b) doesn't have numerical dissipation compared to to steep waves (Fig.25d) with a numerical dissipation of about 6% with respect to FNPT results. Thus, numerical dissipation plays a role and weak or strong coupling from potential based model is ideal. Thus, numerical dissipation plays a role and weak or strong coupling from potential based model is ideal.~~

Formatted: Font color: Accent 1

Commented [MQ3]: As the examples about the computational time have been discussed above

Commented [MQ4]: What method do you use? With or without the physical viscosity?
For Euler based method, the main numerical error comes from convection term. For Lagrangian method or particle method, what is the main source of the numerical dissipation?

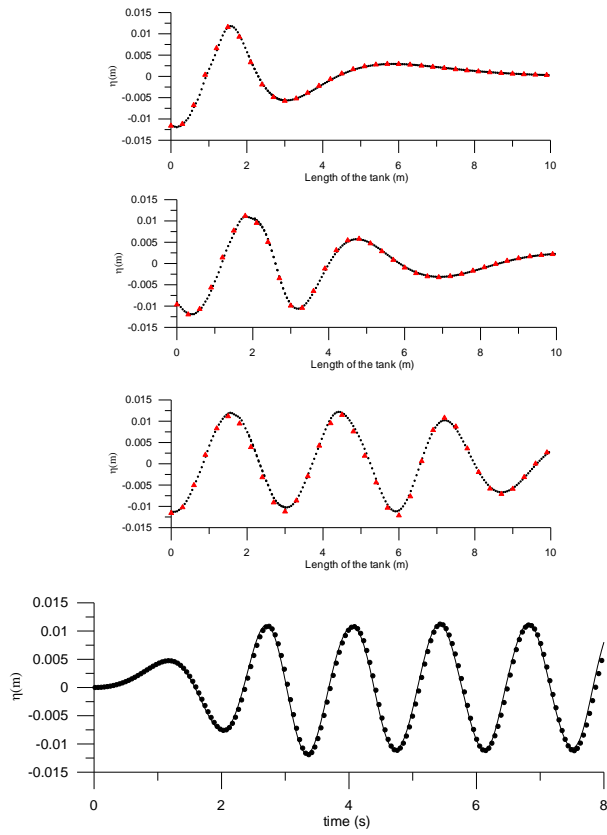


Fig. 12. Comparison between analytical (dot/triangle) and numerical (lines) spatial wave profiles (obtained by using MLPG_R method) at different time instants a) $t = 2s$ b) $t = 4 s$ and c) $t = 8 s$ (d) time history at $x = 4m$.

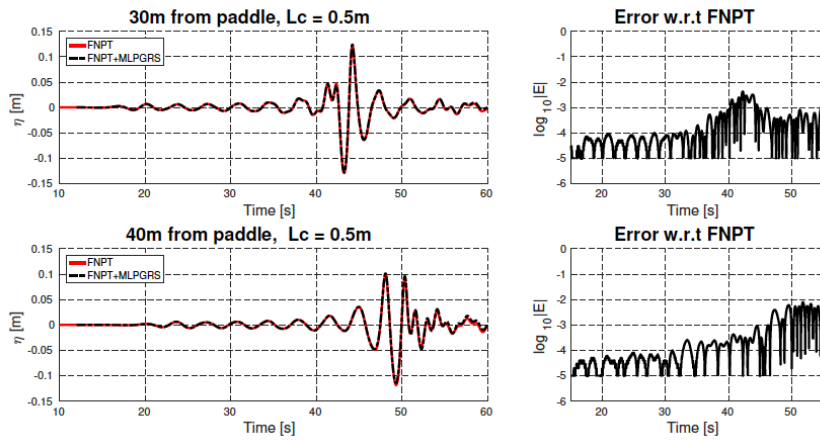


Fig. 13. Focusing wave elevation comparison with FNPT and Shagun et al., (2021) 3D MLPGRS model and the errors.

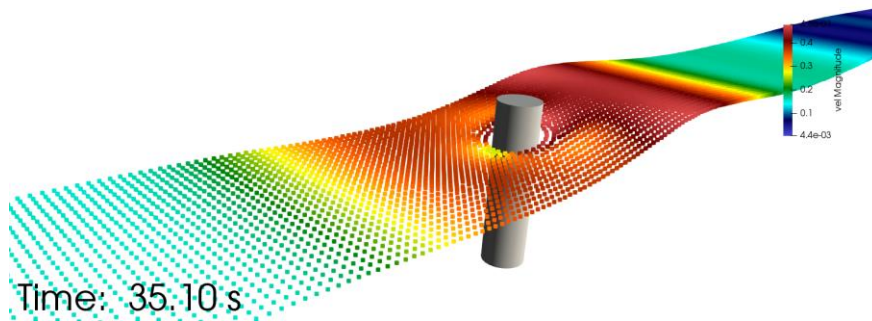


Fig. 14. Non-breaking focused wave interactions with cylinder (Shagun et al., 2021)

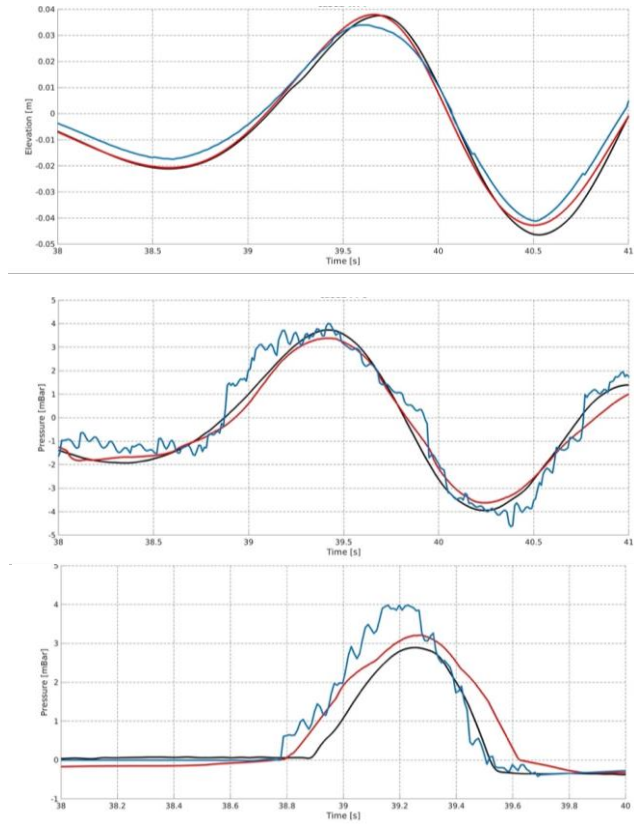


Fig. 15. Comparison between 3D MLPG_RS (Red) and SPH (Blue) with experiments (black) for focused wave – cylinder interactions (extracted from Sriram *et al.*, 2021, comparative study)

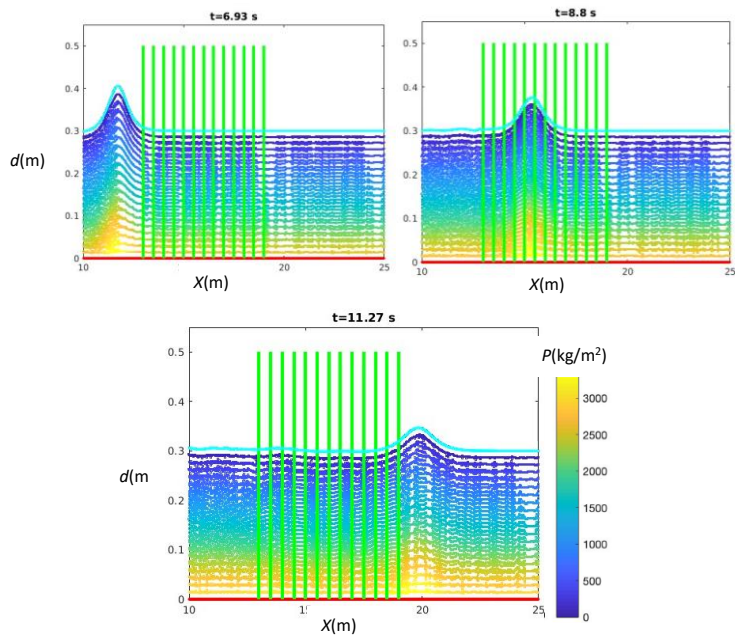


Figure 16. Snapshot of wave propagation along with the pressure contours. The cyan colour shows the free surface. The green colour showing vegetation is only for representative purpose. (Divya *et al.*, 2020)

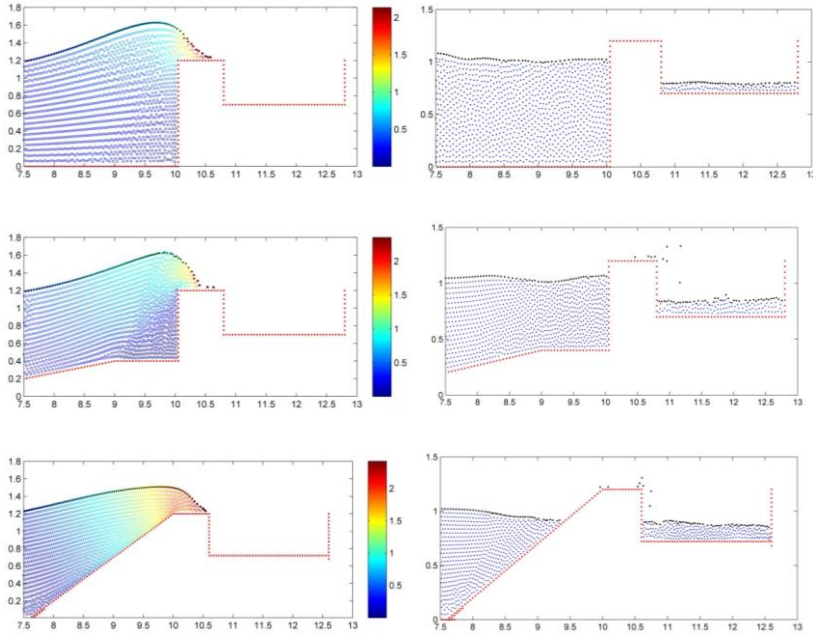


Fig. 17. Overtopping. Left plots: Spatial variations of velocity (magnitude) for different configurations with $H/d = 0.4$, at a same time instant of 4.5s. Right plots: total volume collected at the end of the simulations. (Ma and Sriram, 2015)

Commented [MQ5]: Which one you refer here? I could not find the paper.

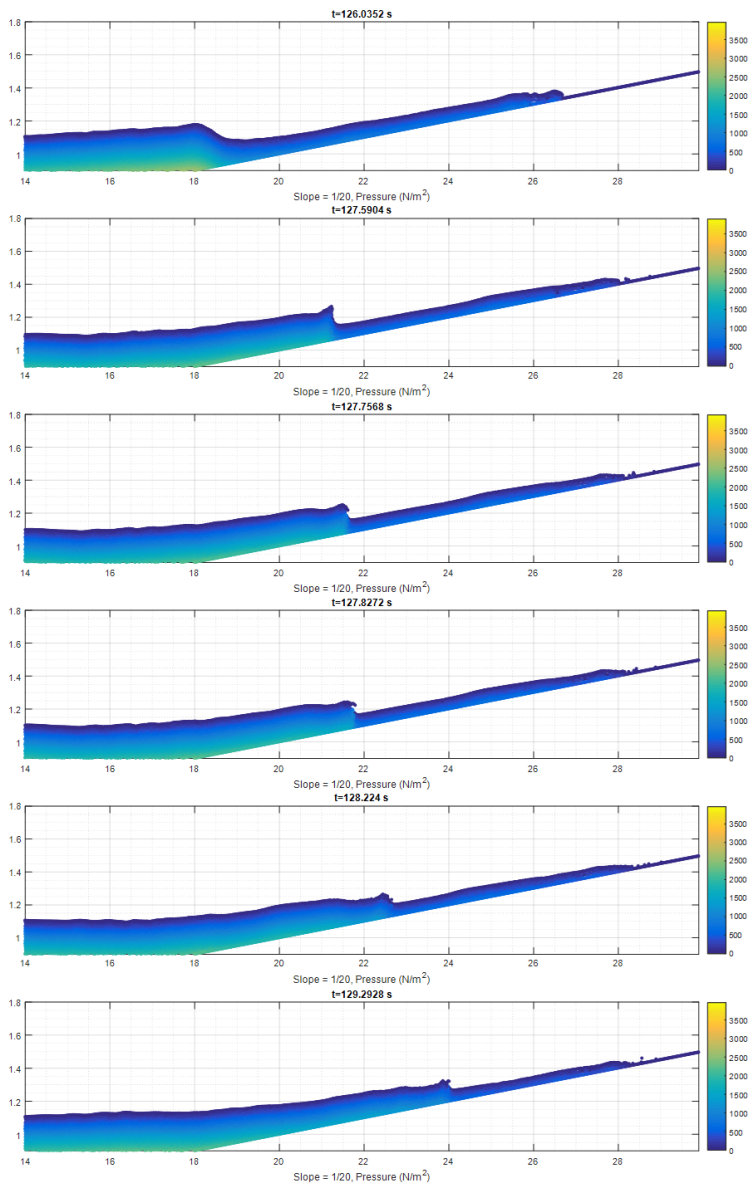


Fig 18: Runup of an undular bore breaking over a slope of 1:20. (Kumar et al., 2021)

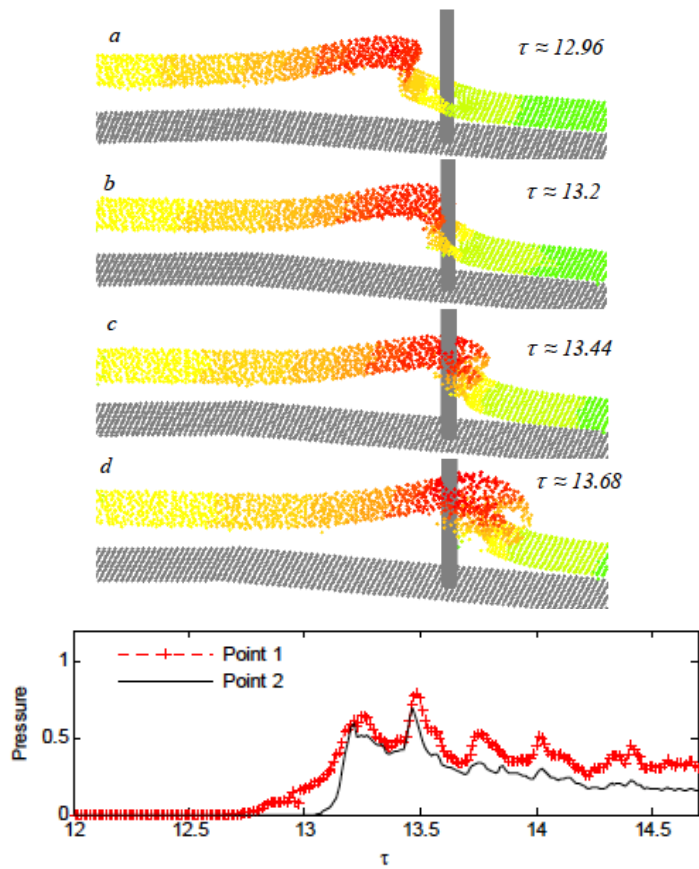
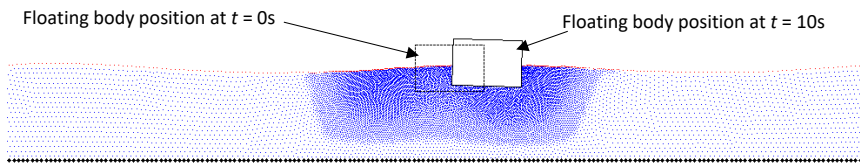
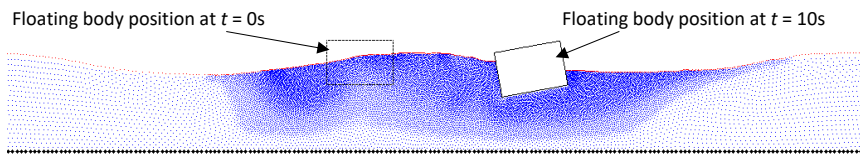


Fig. 19. Different waves profiles of breaking solitary wave impacting on a vertical cylinder (monopile of offshore wind energy) and pressure recording at two locations (Point 1 - 0.1 above MWL; Point 2 - 0.3 above MWL) (Zhou *et al.*, 2009)



(a) Small wave, $H = 0.04\text{m}$ and $T = 1.2\text{s}$



(b) Steep wave, $H = 0.1\text{m}$ and $T = 1.2\text{s}$

Fig. 20. Floating body positions at $t = 0\text{s}$ and $t = 10\text{s}$ for small and steep wave. (Rijas *et al.*, 2019)

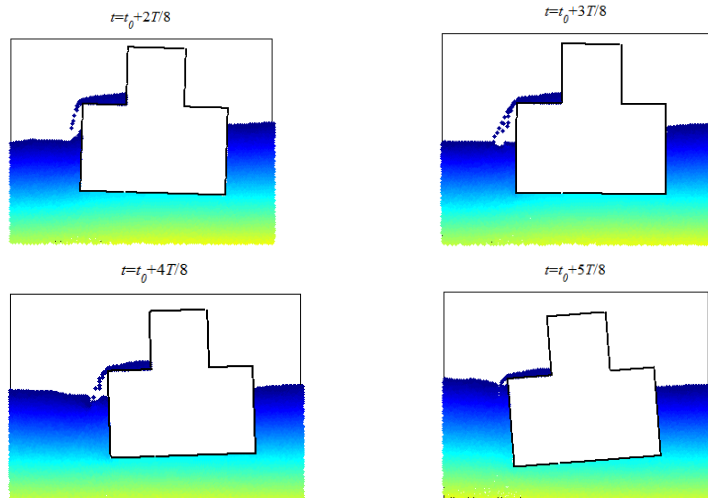


Fig 21. Floating body motion response under green water loading (Rijas *et al.*, 2019)

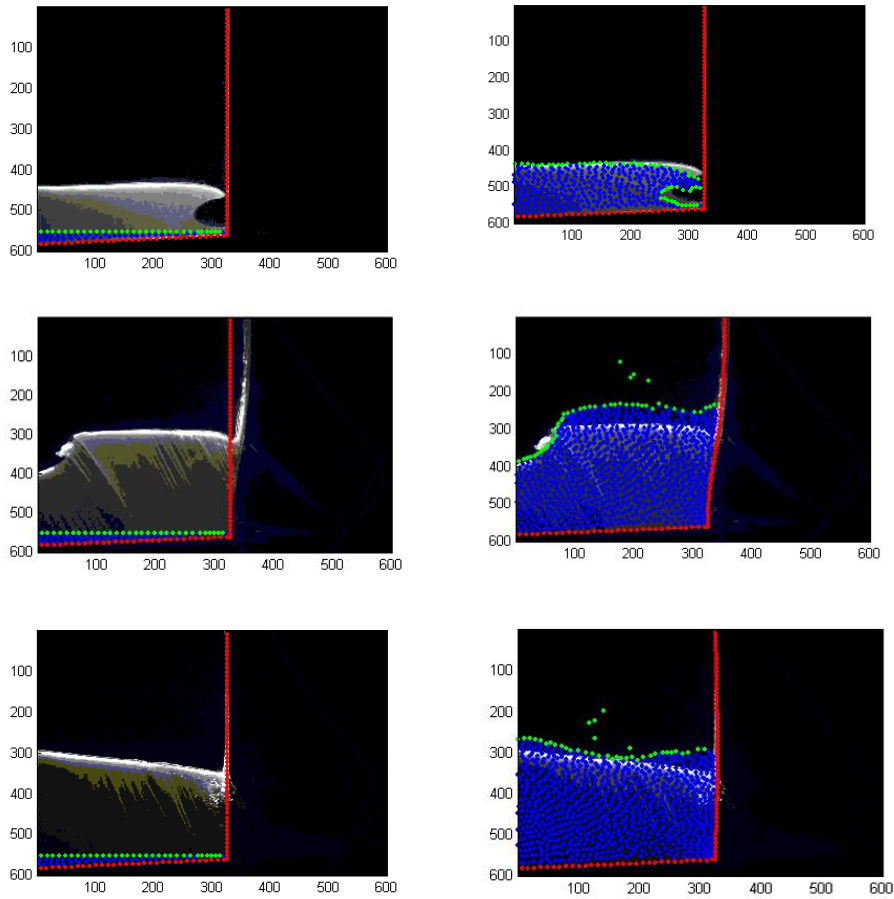


Fig. 22. Comparison between experimental high speed image and numerical model results for solitary wave impact with elastic plate (High speed image obtained from Dr. Oliver Kimmoun, Kimmoun *et al.*, 2009). Left side pictures showing the initial configuration in the numerical model and Right side pictures shows the comparison between numerical and experiments.

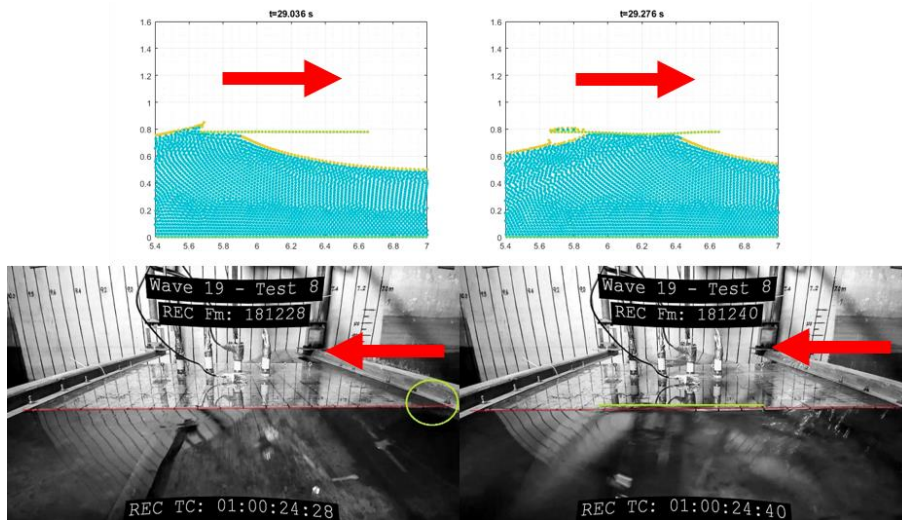
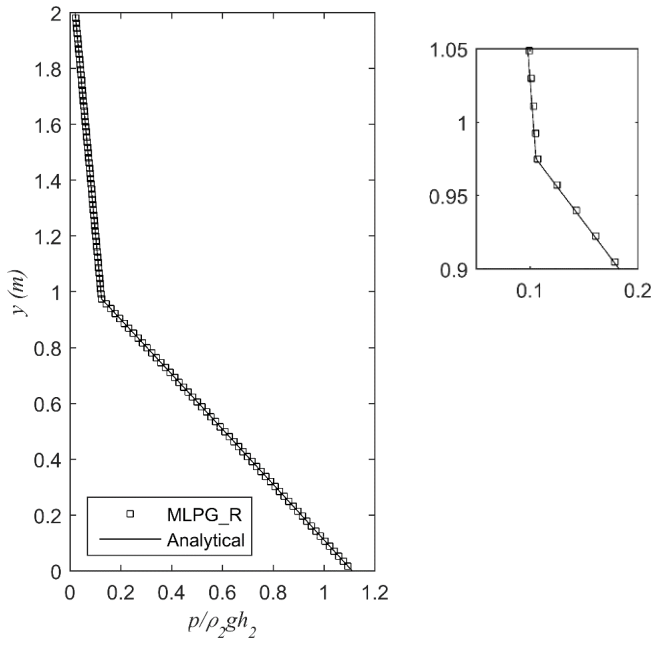
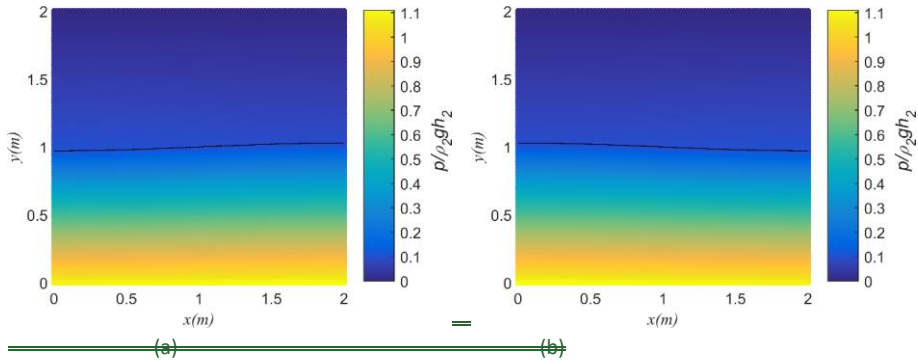


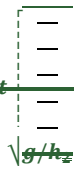
Fig.23. Snapshot of results obtained from the numerical simulation and experiments for focusing waves interacting with the flexible horizontal plate. Highlights show the region of impact and deflection. The red pointer shows the direction of propagation of the wave in experiments and numerical model (Manoj Kumar, 2021).



(c)

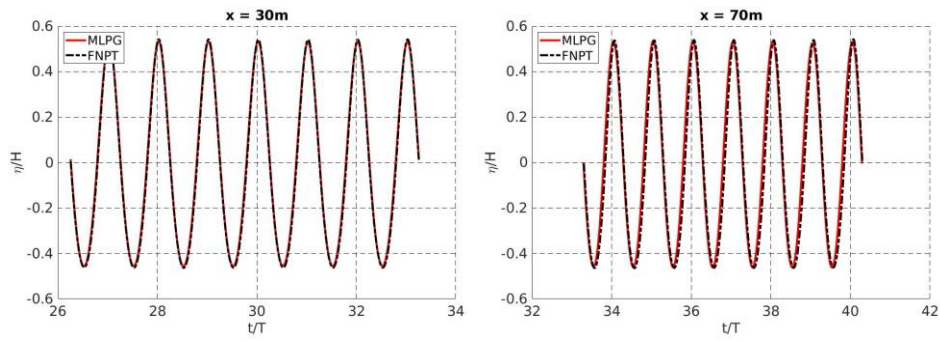
Figure 24: Two phase modelling in a sloshing tank: Snapshots of pressure distribution at the first

quarter ($t\sqrt{g/h_2} = 1.4$) (a) and the third quarter ($t\sqrt{g/h_2} = 1.4$) (b) of the first period with

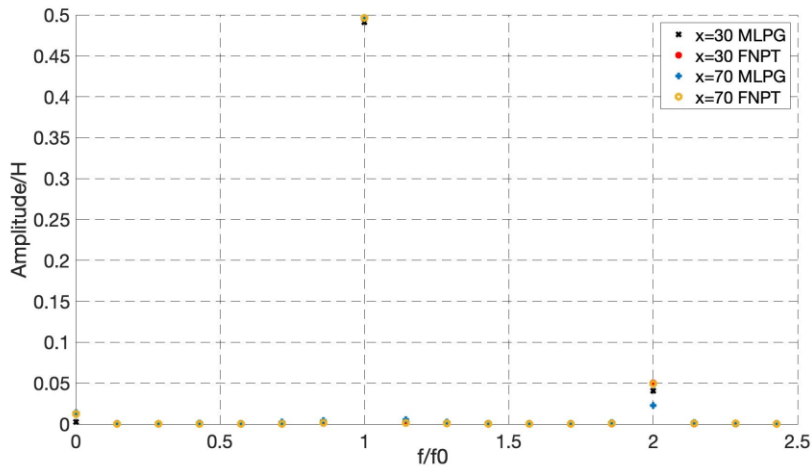


~~interfaces shown in black. (c) Pressure distributions along the depth at $x=0.3m$ for the case with density ratio of 10. (Zhou et al., 2015)~~

(a)



(b)



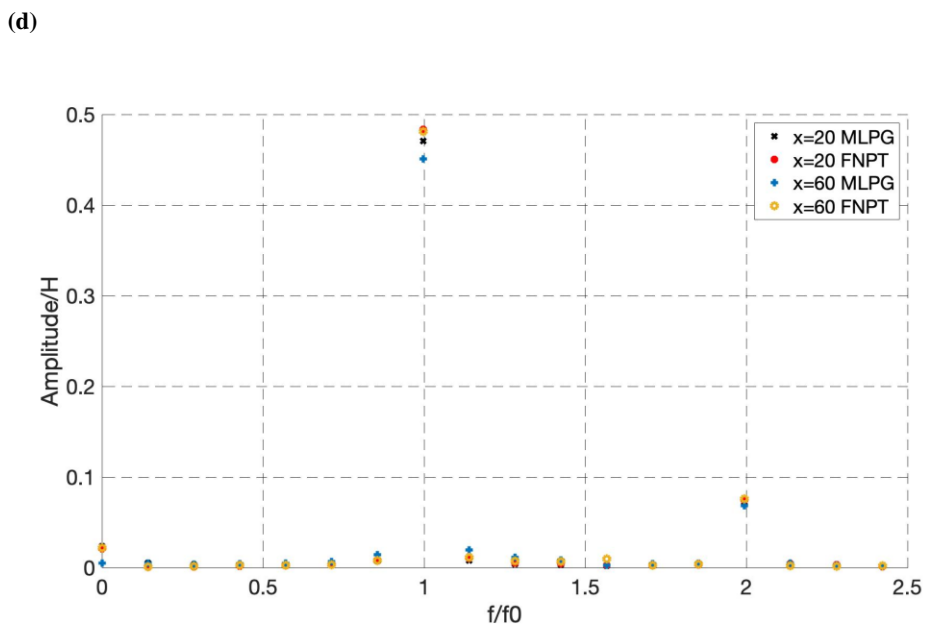
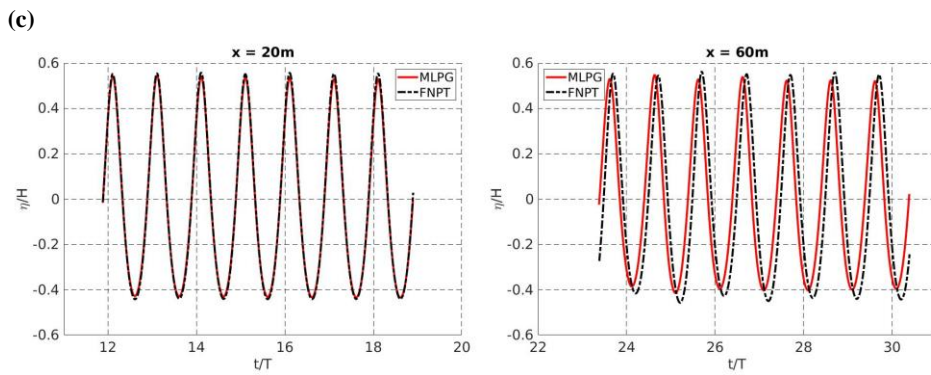
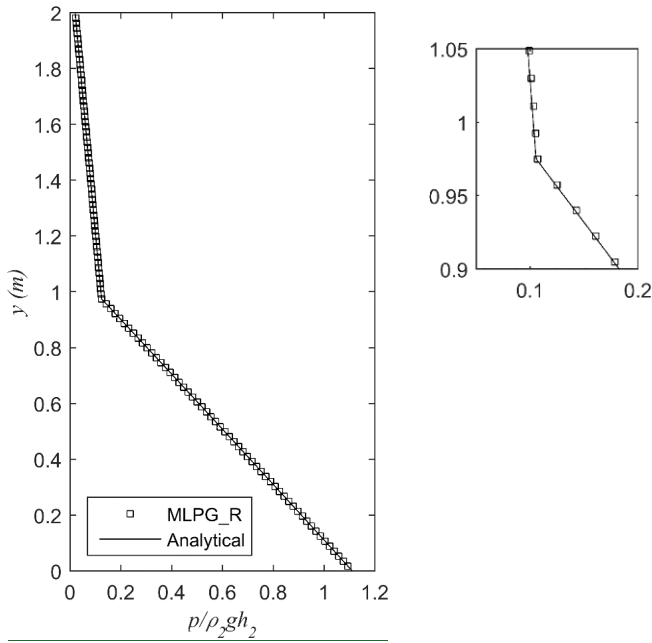
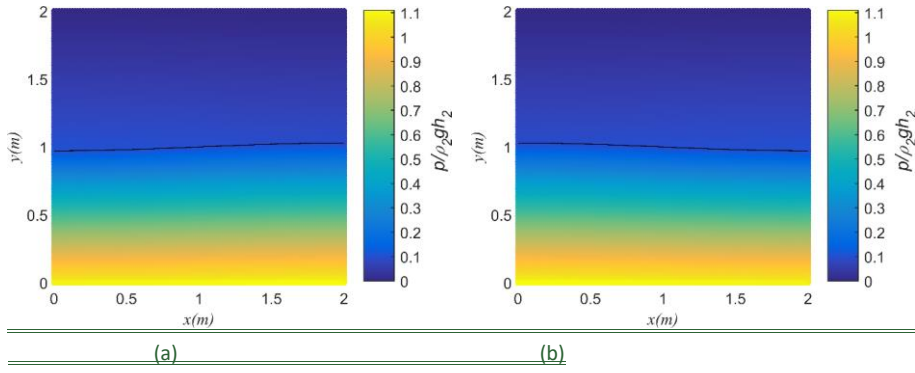


Fig. 2524. (a) Regular wave simulation for smaller steepness at two different probe locations. (b) FFT of (a) (c) Regular wave simulation for higher steepness at two different probe locations. (d) FFT of (c)



(c)

Figure 24: Two phase modelling in a sloshing tank: Snapshots of pressure distribution at the first quarter ($t\sqrt{g/h_2} = 1.4$) (a) and the third quarter ($t\sqrt{g/h_2} = 4.4$) (b) of the first period with interfaces shown in black. (c) Pressure distributions along the depth at $x=0.3m$ for the case with density ratio of 10. (Zhou et al., 2015)

Formatted: Font color: Accent 1

6.0. Key issues and future directions

The concept of MLPG introduced by Prof. Atluri's and co-workers was redeveloped into a form of the MLPG_R method for being able to model a wide variety of applications involving free surface waves in ocean engineering. The developments have overcome many challenges and hindrances. Use of The local weak form approximation with a Rankin Source solution as its test function -has advantages due to because it does not need to deal with derivatives of unknowns in PPE its flexibility in choosing the test functions and reducing the order of continuity requirements. Nevertheless, the method needs to be improvised further in some of the following aspects.

1. *Turbulence and boundary layer*: For some applications, one must model the turbulence and boundary layer effects. So far in developing this method for ocean engineering problem, these effects are assumed to be negligible. They need to be incorporated to widen the scope of the application of the method. It should be noted that usage of turbulence closure is problem - dependent, applying turbulence for the problems that are not required may lead to lower accuracy than without considering it.

2. *Variable Particle Resolution*: The region with fine node distribution that is required for some problems, such as those about floating structures the range of structure movement, is not easy to estimate at the beginning of the simulations for many problems. However, presently we do it based on the trial or error method. As we already know the wave characteristics and may have a reasonable estimate on how much the body surge. Using the knowledge, we can determine the initial region with fine adopt the initial node distribution accordingly. This is more or less a same issue for all methods which adopt the approach. This need to be investigated and to develop more robust technique to deal with issue.

3. *Breaking waves in 3D and their interactions with 3D floating bodies*: Although some attempts have been made to model this kind of problems, there are still some numerical issues, particularly those arising from the irregular particle distribution near the bodies. Modelling 3D floating bodies requires variably-spaced particle distribution, particularly to capture the fluid dynamics near floating bodies accurately. This is not easy for particle methods. In addition, implementation of variable time steps should also be attempted as the fluid and floating bodies usually have different time-varying properties. Further, better treatment of wall boundary conditions should be attempted for modelling interaction between breaking waves and floating bodies.

4. *Particle shifting strategy*: One of the major hindrances in 3D breaking waves and their interaction with fixed/floating bodies is the irregular particle distribution. This has been rectified in 2D application using a minimum pressure in estimating its gradient (a kind of particle shifting) and interpolating the velocity to these stabilised nodal position. However for 3D applications, the Lagrangian motion of the particles in and near the 3D wake region of a structure may lead to

Formatted: Font color: Accent 1

Commented [MQ6]: The reason I change this because we need to summarise the main feature of MLPG_R, not MLPG in general.

Formatted: Font color: Accent 1

Formatted: Font color: Accent 1

a void. ~~Since, the~~The minimum pressure based estimation to find the nodal position fails in 3D. Based on our experience, the methods that work in other particle methods such as SPH fail in the MLPG_R method. ~~T~~he reason is unclear as of now, but should be investigated further. Novel and robust techniques need to be developed to reduce irregularity of particle distribution.

5. *Computational aspects:* Even though the method works well, the code is largely in serial version so far, just with some subroutines converted to OpenMP. Hence, in future GPU or MPI needs to be implemented in the MLPG_R method and the FNPT model. Thus, the hybrid approach will be much faster.

6. *Benchmark studies:* All numerical model developments and improvements should be validated against the experimental observations. The MLPG_R method has been not only validated for small scale but also large scale experiments for wave propagation, interactions with structures and runup. Nevertheless, the method needs to be further validated for many other complex cases, such as two-phase wave impact in large scale and breaking wave interaction with 3D rigid and flexible structures.

7. *3D Coupling:* Coupling the NS solver with Potential flow/Euler solvers brings in benefits at least in two folds. One is to tackle the problems of numerical damping of the NS solvers with modelling long distance and long duration propagation of nonlinear water waves. The another is to reduce computational time. Although computational time would be relative less important once the next generation of computers (such as quantum computers) are coming up, the reduction of computational time is still of a great benefit for practical use at this moment and in years to come. As reviewed above, coupling with different solvers has been successfully implemented in the recent years, but most of the work deals with 2D problems. A full two-way coupling of different solvers for modeling real 3D problems in particle method has not been attempted to the best of our knowledge. There are many challenges in 3D coupling. A few are indicated here. One of them is that a surface- based transformation of variables between solvers in coupling region may fail in 3D cases due to wave directionality and the complexity of waves induced by 3D floating bodies. Better techniques need to be developed for 3D modelling. Another one is associated with overlapping zones. They are predefined at the beginning of the simulations based on the input wave characteristics. This is considered as a limitation for modelling 3D floating bodies in waves with potential large motions, as the predefined overlapping zones may not be appropriate at the later stage. Moreover, in the existing works, overlapping zones are assumed not to be in the region with any breaking events. The authors are unaware of the methodology to remove this limitation now, but we envisage that the future studies may eliminate the limitation. Further, new coupling strategies need to be sought for 3D cases except splitting the domain into two parts as in 2D cases. For example, embedding a small NS domain (spherical or cuboidal domain) into a large potential model domain needs information exchange on the whole boundary surface surrounding the NS domain. One-way coupling of such a strategy is relatively easier but two-way coupling will be a big challenge. [Apart from domain based decomposition, implementation of functional splitting in particle](#)

method should be attempted such as [in SWENSE-mesh-based method](#) (Li et al., 2021 [and Li, 2017](#)), wherein potential and viscous flow decomposition has been used.

7.0. Acknowledgement

The first author would like to thank DST-INSPIRE, DST-UKIERI, Newton International fellowship, AvH fellowship for funding the development of MLPG for wide variety of applications. Many fruitful discussion with Dr. Shiqiang Yan by the first author in FNPT and NS. These developments are not feasible without the help of Dr. Juntao Zhou, Dr. Rijas, Dr. Manoj kumar, Mr. Shagun, Mr. Vineesh and Mrs. Divya for their support in improving the MLPG model capabilities.

8.0. References

1. Akbari, H and Namin, MM, (2013). Moving particle method for modeling wave interaction with porous structures. *Coastal Engineering*. 74, 59-73.
2. Akbari, H and Pooyarad, A, (2020). Wave force on protected submarine pipelines over porous and impermeable beds using SPH numerical model. *Applied Ocean Research*. 98, 102118.
3. Akbari, H and Taherkhani, A, (2019). Numerical study of wave interaction with a composite breakwater located on permeable bed. *Coastal Engineering*. 146, 1-13.
4. Altomare, C, Domínguez, J, Crespo, A, Suzuki, T, Caceres, I and Gómez-Gesteira, M, (2015). Hybridization of the wave propagation model SWASH and the meshfree particle method SPH for real coastal applications. *Coastal Engineering Journal*. 57 (4), 1550024-1-1550024-34.
5. Atluri, S. N. and Shen, S. (2002) The Meshless Local Petrov-Galerkin (MLPG) method: A simple & less-costly alternative to the finite element and boundary element methods, *CMES - Computer Modeling in Engineering and Sciences*, 3, 11–51.
6. Atluri, S. N., Han, Z. D., Rajendran, A. M. (2004). A new implementation of the meshless finite volume method, through the MLPG ‘mixed’ approach. *CMES - Computer Modeling in Engineering and Sciences*. 6: 491–513.
7. Atluri, S. N., Liu, H. T., Han, Z. D. (2006a). Meshless Local Petrov-Galerkin (MLPG) mixed collocation method for elasticity problems. *CMES - Computer Modeling in Engineering and Sciences*. 14:141–152.
8. Atluri, S. N., Liu, H. T., Han, Z. D. (2006b). Meshless Local Petrov-Galerkin (MLPG) mixed finite difference method for solid mechanics. *CMES - Computer Modeling in Engineering and Sciences*. 15: 1–16.
9. Atluri, S.N., Zhu, T., (1998). A new meshless local Petrov-Galerkin (MLPG) approach in computational mechanics. *Computational Mechanics*. 22:117-127.
10. Attaway, S.W., Heinstejn, M.W., Swegle, J.W., (1994). Coupling of smooth particle hydrodynamics with the finite element method. *Nucl. Eng. Des.* 150, 199–205. [https://doi.org/10.1016/0029-5493\(94\)90136-8](https://doi.org/10.1016/0029-5493(94)90136-8)
11. Barecasco, A., Terissa, H., Naa, C.F., (2013). Simple free-surface detection in two and three-dimensional SPH solver. *ArXiv Prepr.* <https://arxiv.org/abs/1309.4290>

12. Belytschko, T., Lu, Y.Y., Gu, L. (1994). Element-free Galerkin methods. *Int J Numer Methods Eng.* 37:229-256.
13. Brinkman, H. C., (1947). A calculation of the viscous force exerted by a flowing fluid on a dense swarm of particles, *Appl. Sci. Res.* 27–34
14. Chorin, A. J. (1968). Numerical solution of the Navier-Stokes equations. *Math Comput.* 22:745-762.
15. Colagrossi, A and Landrini, M, (2003). Numerical simulation of interfacial flows by smoothed particle hydrodynamics. *Journal of Computational Physics.* 191 (2), 448-475.
16. Dao, MH (2010). Numerical study of plunging wave in deep water. Ph.D. Thesis, National University of Singapore
17. Divya, R., Sriram, V., (2017). Wave-porous structure interaction modelling using Improved Meshless Local Petrov Galerkin method. *Applied Ocean Research.* 67, 291–305.
18. Divya, R., Sriram, V., Murali, K. (2020). Wave-vegetation interaction using Improved Meshless Local Petrov Galerkin method. *Appl. Ocean Res.* 101,102116
19. Duan, G, Yamaji, A and Sakai, M, (2020). An incompressible–compressible Lagrangian particle method for bubble flows with a sharp density jump and boiling phase change. *Computer Methods in Applied Mechanics and Engineering.* 372, 113425.
20. Farhat, C., Lesoinne, M., LeTallec, P. (1998). Load and motion transfer algorithms for fluid/structure interaction problems with nonmatching discrete interfaces: Momentum and energy conservation, optimal discretization and application to aeroelasticity. *Comput. Methods Appl. Mech. Eng.* 157: 95–114.
21. Fonty, T, Ferrand, M, Leroy, A and Violeau, D, (2020). Air entrainment modeling in the SPH method: a two-phase mixture formulation with open boundaries. *Flow, Turbulence and Combustion.* 105, 1149-1935 1195.
22. Fourey, G, Hermange, C, Le Touzé, D and Oger, G, (2017). An efficient FSI coupling strategy between Smoothed Particle Hydrodynamics and Finite Element methods. *Computer Physics Communications.* 217, 66-81.
23. Fourtakas, G, Stansby, P, Rogers, B, Lind, S, Yan, S and Ma, Q, (2018). On the coupling of 1943 incompressible SPH with a finite element potential flow solver for nonlinear free-surface flows. *1944 International Journal of Offshore and Polar Engineering.* 28 (3), 248-254.
24. He, G., M. Khasiwagi, and C. Hu (2009) Nonlinear Solution for Vibration of Vertical Elastic Plate by Initial Elevation of Free Surface, In *Proceedings of the Nineteenth (2009) International Offshore and Polar Engineering Conference, Osaka, Japan, June 21-26, 406-413.*
25. Gong, J., Yan, S., Ma, QW, Li Y. (2020), ‘Added resistance and seakeeping performance of trimarans in oblique waves’, *Ocean Engineering* 216 (2020) 107721.
26. Gotoh H and Khayyer A (2016) Current achievements and future perspectives for projection-based particle methods with applications in ocean engineering, *J. Ocean Eng. Mar. Energy,* 2 (3), 251-278
27. Gotoh H and Khayyer A (2018) On the state-of-the-art of particle methods for coastal and ocean engineering. *Coastal Engineering Journal,* 60:79-103
28. Grenier, N, Le Touzé, D, Colagrossi, A, Antuono, M and Colicchio, G, (2013). Viscous bubbly flows simulation with an interface SPH model. *Ocean Engineering.* 69, 88-102.
29. Grilli, S. T., Gilbert, R., Lubin, P., Vicent, S., Legendre, D., Duyam, M., Kimmoun, O., Branger, H., Devrard, D., Fraunie, P., Abadie, S. (2004). Numerical modeling and experiments for solitary wave shoaling and breaking over a sloping beach. In: *Proceedings of*

- the Fourteenth (2004) International Offshore and Polar Engineering Conference, Toulon, France, pp. 306–312.
30. Grilli, S. T., Guyenne, P., Dias, F. (2001). A fully non-linear model for three dimensional overturning waves over an arbitrary bottom. *Int J Numer Methods Fluids*. 35(7):829–67. doi:10.1002/1097-0363(20010415)35:7<829:AID-FLD115>3.0.CO;2-2
 31. Grilli, S.T. (2008) *On the Development and Application of Hybrid Numerical Models in Nonlinear Free Surface Hydrodynamics*. Keynote lecture in Proc. 8th Intl. Conf. on Hydrodynamics (Nantes, France, September 2008) (P. Ferrant and X.B. Chen, eds.), 21-50.
 32. Harlow, F. H., Welch, J. E. (1965) Numerical calculation of time-dependent viscous incompressible flow of fluid with free surface. *Physics of Fluids*. 8: 2182–2189.
 33. Hirt, C. W., Nichols, B. D. (1981). Volume of fluid (VOF) method for the dynamics of free boundaries. *J. Comput. Phys.* 39:201–225. doi:10.1016/0021-9991(81)90145-5.
 34. Idelsohn, S., Oate, E., Pin, F. D. (2004). The particle finite element method: a powerful tool to solve incompressible flows with free-surfaces and breaking waves. *Int J Numer Methods Eng.* 61(7):964–89. doi:10.1002/nme.1096.
 35. Irons, B., Tuck, R. C. (1969). A version of the Aitken accelerator for computer implementation, *Int. J. Numer. Methods Eng.* 1: 275–277.
 36. Isshiki H.(2011) Discrete differential operators on irregular nodes (DDIN) *Internat. J. Numer. Methods Engrg.*, 88 (2011), 1323-1343
 37. J. Bonet and T.S. Lok (1999) Variational and momentum preservation aspects of smooth particle hydrodynamic formulation. *Comput Methods Appl Mech Engg*, 180 :97-115
 38. Johnson, G.R., (1994). Linking of Lagrangian particle methods to standard finite element methods for high velocity impact computations. *Nucl. Eng. Des.* 150, 265–274. [https://doi.org/10.1016/0029-5493\(94\)90143-0](https://doi.org/10.1016/0029-5493(94)90143-0)
 39. Kassiotis C., Ferrand M., Violeau D., and Rogers B.D. (2011) Coupling SPH with a 1-D Boussinesq-type wave model, 6th International SPHERIC Workshop, Hamburg, Germany.
 40. Khayyer A, Gotoh H, Shao S.D. (2008). Corrected Incompressible SPH method for accurate water-surface tracking in breaking waves. *Coastal Engineering*, 55 (3):236-250
 41. Khayyer A, Gotoh H., (2010). A higher order Laplacian model for enhancement and stabilization of pressure calculation by the MPS method., *Applied Ocean Research*, 32 (1): 124-131.
 42. Khayyer, A and Gotoh, H, (2016). A multiphase compressible-incompressible particle method for water slamming. *International Journal of Offshore Polar Engineering*. 26 (01), 20-25.
 43. Khayyer, A, Gotoh, H, Falahaty, H and Shimizu, Y, (2018). An enhanced ISPH–SPH coupled method for simulation of incompressible fluid–elastic structure interactions. *Computer Physics Communications*. 232, 139-164.
 44. Khayyer, A., Gotoh, H and Shao S (2009). Enhanced predictions of wave impact pressure by improved incompressible SPH methods. *Applied Ocean Research* 31 (2):111–131.
 45. Koo, W., Kim, M. H. (2004). Freely floating-body simulation by a 2D fully nonlinear numerical wave tank, *Ocean Eng.* 31:2011–2046. doi:10.1016/j.oceaneng.2004.05.003.
 46. Koshizuka, S, Tamako, H and Oka, Y, (1995). A particle method for incompressible viscous flow with fluid fragmentation. *Computational Fluid Dynamics Journal*. 4 (1), 29-46.
 47. Koshizuka, S., Nobe, A., Oka, Y. (1998). Numerical analysis of breaking waves using the moving particle semi-implicit method. *Int J Numer Methods Fluids*. 26:751-769.

48. Koshizuka, S., Oka, Y. (1996). Moving-particle semi-implicit method for fragmentation of incompressible fluid. Nucl Sci Eng. 123:421-434.
49. Li Q, Wang J, Yan S, Gong J, Ma Q (2018), 'A zonal hybrid approach coupling FNPT with OpenFOAM for modelling wave-structure interactions with action of current', Ocean Systems Engineering 8(4):381-407.
- 49-50. Li, Qian (2017), 'a hybrid model based on functional decomposition for vortex shedding simulations', PhD thesis, City University of London.
- 50-51. Li, Z., Bouscasse B., Ducroz G., Gentaz L., Le Touze' D, Ferrant P., (2021) Spectral Wave Explicit Navier-Stokes Equations for wave-structure interactions using two-phase Computational Fluid Dynamics solvers, Ocean Engineering, 221. <https://doi.org/10.1016/j.oceaneng.2020.108513>.
- 51-52. Lin, H., Atluri, S. N. (2001). The meshless local Petrov-Galerkin (MLPG) method for solving incompressible Navier-Stokes equations. Comput Model Eng Sci. 2:117-142.
- 52-53. Lind SJ, Rogers BD, Stansby PK. (2020). Review of smoothed particle hydrodynamics: towards converged Lagrangian flow modelling. Proc. R. Soc. A, 476:20190801. <http://dx.doi.org/10.1098/rspa.2019.0801>.
- 53-54. Lind, SJ, Stansby, PK and Rogers, BD, 2016. Incompressible-compressible flows with a transient discontinuous interface using smoothed particle hydrodynamics (SPH). Journal of Computational Physics. 309, 129-147.
- 54-55. Lind, SJ, Stansby, PK, Rogers, BD and Lloyd, PM, 2015. Numerical predictions of water-air wave slam using incompressible-compressible smoothed particle hydrodynamics. Applied Ocean Research. 2237 49, 57-71.
- 55-56. Liu, W.K., Chen, Y., Jun, S. (1996). Overview and applications of the reproducing Kernel particle methods. Arch Comput Methods Eng. 3:3-80.
- 56-57. Lo, EYM and Shao, S, 2002. Simulation of near-shore solitary wave mechanics by an incompressible SPH method. Applied Ocean Research. 24 (5), 275-286.
- 57-58. Long, T, Hu, D, Wan, D, Zhuang, C and Yang, G, 2017. An arbitrary boundary with ghost particles incorporated in coupled FEM-SPH model for FSI problems. Journal of Computational Physics. 350, 166-183.
- 58-59. Luo M., Khayyer A., Lin P (2021). Particle methods in ocean and coastal engineering, Accepted for publication in Applied Ocean Research.
- 59-60. Luo, M, Koh, CG, Bai, W and Gao, M, 2016. A particle method for two-phase flows with compressible air pocket. International Journal for Numerical Methods in Engineering. 108 (7), 695-721.
- 60-61. Ma QW, Wu GX, and Eatock Taylor R. Finite element simulation of fully non-linear interaction between vertical cylinders and steep waves. Part 1: Methodology and numerical procedure. International Journal for Numerical Methods in Fluids, 36(3), (2001) 265-285.
- 61-62. Ma QW, Zhou Y, Yan S. (2016). A review on approaches to solving Poisson's equation in projection-based meshless methods for modelling strongly nonlinear water waves. J. Ocean Eng. Mar. Energy, 2, 279-299.
- 62-63. Ma, Q. W. (2005). MLPG method based on Rankine source solution for simulating nonlinear water waves. Comput Model Eng Sci. 9:193-209.
- 63-64. Ma, Q. W. (2008). A new meshless interpolation scheme for MLPG_R method. Comput Model Eng Sci. 23:75-90.
- 64-65. Ma, Q.W., 2005. Meshless local Petrov-Galerkin method for two-dimensional nonlinear water wave problems. J. Comput. Phys. 205, 611-625.

Formatted: Font color: Accent 1

Formatted: Font color: Accent 1

- [65-66.](#) Ma, Q.W., Zhou, J. T. (2009). MLPG_R method for numerical simulation of 2D breaking waves. *Comput Model Eng Sci.* 43:277-303.
- [66-67.](#) Ma, QW and Yan, S, 2006. Quasi ALE finite element method for nonlinear water waves. *Journal of 2312 Computational Physics.* 212 (1), 52-72.
- [67-68.](#) Manoj Kumar G., (2021). A Hybrid Numerical model for simulating wave structure interaction., PhD Thesis, IIT Madras, India.
- [68-69.](#) Manoj Kumar, G., Sriram, V. (2016). A hybrid numerical model to address fluid elastic structure interaction. Proceedings of the International Conference on Offshore Mechanics and Arctic Engineering – OMAE 2016, Busan, South Korea.
- [69-70.](#) Manoj Kumar, G., Sriram, V. (2017). Improved hybrid numerical model for fluid-elastic structure interaction using FEM and MLPG-R. 27th International Ocean and Polar Engineering Conference, ISOPE 2017, San Francisco, United States. 696-703.
- [70-71.](#) Manoj Kumar, G., Sriram, V., (2020). Development of a hybrid model based on Mesh and Meshfree methods and its application to fluid-elastic structure interaction, *Journal of Fluids and Structures.* 99:103159.
- [71-72.](#) Manoj Kumar, G., Sriram, V., Didenkulova, I. (2020). A hybrid numerical model based on FNPT-NS for the estimation of long wave run-up. *Ocean Eng.* 202:107181, <https://doi.org/10.1016/j.oceaneng.2020.107181>.
- [72-73.](#) Marrone, S., Antuono, M., Colagrossi, A., Colicchio, G., Le, Touzé, D., Graziani, G. (2011). δ -SPH model for simulating violent impact flows. *Comput Methods Appl Mech Eng.* 200:1526-1542.
- [73-74.](#) Marrone, S., Colagrossi, A., Antuono, M., Lugni, C., Tulin, M. P. (2011). A 2D+t SPH model to study the breaking wave pattern generated by fast ships. *J Fluids Struct.* 27:1199-1215.
- [74-75.](#) Monaghan J.J (2012). Smoothed Particle Hydrodynamics and Its Diverse Applications, *Annual Review of Fluid Mechanics*, 44:323-346.
- [75-76.](#) Monaghan, J. J. (1988). An introduction to SPH. *Computer Physics Communications.* 48:89–96.
- [76-77.](#) Monaghan, J.J, 1994. Simulating free surface flows with SPH. *Journal of Computational Physics.* 110 (2), 399–406.
- [77-78.](#) Mukherjee YX, Mukherjee S (1997) On boundary conditions in the element-free Galerkin method. *Computational Mechanics*, 19, 264-270.
- [78-79.](#) Nakayama, T., Washizu, K. (1981). The boundary element method applied to the analysis of two-dimensional nonlinear sloshing problems. *International Journal for Numerical Methods in Engineering.* 17:1631–1646.
- [79-80.](#) Narayanaswamy M, Crespo AJC, Gomez-Gesteira M., and Dalrymple R.A. (2010) SPHysics-FUNWAVE hybrid model for coastal wave propagation, *J. of Hydraulic Research*, 48, 85-93.
- [80-81.](#) Nayroles, B., Touzot, G., Villon, P. (1992). Generalizing the finite element method: diffuse approximation and diffuse elements. *Computational Mechanics.* 10:307-318.
- [81-82.](#) Neuman, S. P., Witherspoon, P. A. (1970). Finite element method of analyzing steady seepage with a free surface. *Water resources research.* 6:889–897.
- [82-83.](#) Ng K.C., Hwang Y.H., Sheu T.W.H. (2014) On the accuracy assessment of Laplacian models in MPS, *Comput. Phys. Comm.*, 185 (2014), 2412-2426

- ~~83-84.~~ Ni, X, Feng, W, Huang, S, Zhao, X and Li, X, 2020b. Hybrid SW-NS SPH models using open boundary conditions for simulation of free-surface flows. *Ocean Engineering*. 196, 106845.
- ~~84-85.~~ O. Kimmoun, S. Malenica, Y.M. Scolan (2009), Fluid structure interactions occurring at a flexible vertical wall impacted by a breaking wave. In Proceedings of the Nineteenth International Offshore and Polar Engineering Conference, Osaka, Japan, June 21-26. 3: 308-315.
- ~~85-86.~~ Omidvar, P., Stansby, P. K. Rogers BD. (2013). SPH for 3D floating bodies using variable mass particle distribution. *Int J Numer Methods Fluids*. 72:427-452.
- ~~86-87.~~ Omidvar, P., Stansby, P. K., Rogers, B. D. (2012). Wave body interaction in 2D using smoothed particle hydrodynamics (SPH) with variable particle mass. *Int J Numer Methods Fluids*. 68:686-705.
- ~~87-88.~~ Rafiee, A and Thiagarajan, KP, 2009. An SPH projection method for simulating fluid-hypoelastic 2476 structure interaction. *Computer Methods in Applied Mechanics and Engineering*. 198 (33-36), 2785-2477 2795.
- ~~88-89.~~ Rafiee, A, Dutykh, D and Dias, F, 2015. Numerical simulation of wave impact on a rigid wall using a two-phase compressible SPH method. *Procedia IUTAM*. 18, 123-137.
- ~~89-90.~~ Ravindar et al., 2022
- ~~90-91.~~ Ren, B, Wen, H, Dong, P and Wang, Y, 2016. Improved SPH simulation of wave motions and turbulent flows through porous media. *Coastal Engineering*. 107, 14-27.
- ~~91-92.~~ Rijas, A. S., Sriram, V. (2019). Numerical modelling of forced heaving of mono hull and twin hull in particle method. *Ocean Engineering*. 173:197-214.
- ~~92-93.~~ Rijas, A. S., Sriram, V., Yan, S. (2019). Variable spaced particle in meshfree method to handle wave-floating body interactions, *International Journal for Numerical Methods in Fluids*. 91: 263-286.
- ~~93-94.~~ Rogers, B., Dalrymple, R., Stansby, P. (2009). Simulation of caisson breakwater movement using 2-D SPH, *J. Hydraul. Res.* 47:135-141.
- ~~94-95.~~ Shagun, A., Sriram, V., Yan, S., Murali, K. (2021). Improvements in MLPG formulation for 3D wave interaction with fixed structures, *Computers and Fluids*. 218.
- ~~95-96.~~ Shi, Y, Li, S, Chen, H, He, M and Shao, S, 2018. Improved SPH simulation of spilled oil contained by flexible floating boom under wave-current coupling condition. *Journal of Fluids and Structures*. 76, 272-300.
- ~~96-97.~~ Shimizu, Y, Khayyer, A, Gotoh, H and Nagashima, K, 2020. An enhanced multiphase ISPH-based method for accurate modeling of oil spill. *Coastal Engineering Journal*. 62 (4), 625-646.
- ~~97-98.~~ Sitanggang K.I Boussinesq-Equation and RANS hybrid wave model, Ph.d thesis, Texas A&M university, USA. (2008)
- ~~98-99.~~ Souto-Iglesias, A., F. Macià, L.M. González, J.L. Cercos-Pita, (2014) Addendum to "On the consistency of MPS" *Computer Physics Communications*, 185(2),595-598
- ~~99-100.~~ Souto-Iglesias, A., F. Macià, L.M. González, J.L. Cercos-Pita, (2013) On the consistency of MPS, *Comput. Phys. Commun.*, 184 (2013), pp. 732-745
- ~~100-101.~~ Sriram V, Agarwal S, Yan S, Xie Z, Saincher S, Schlurmann T, Ma Q W, Stoesser T, Zhuang Y, Han B, Zhao W, Yang X, Li Z, Wan D, Zhang Y, Teng B, Ning D, Zhang N, Zheng X, Xu G, Gong J, Li Y, Liao K, Duan W, Han R, Asnim W, Sulaiman Z, Zhou Z, Qin J, Li Y, Song Z, Lou X, Lu L, Yuan C, Ma Y, Ai C, Dong G, Sun H, Wang Q, Zhai Z-T, Shao Y-L, Lin Z, Qian L, Bai W, Ma Z, Higuera P, Buldakov E, Stagonas D,

- Lopez S M, Christou A, Lin P, Li Y, Lu J, Hong S Y, Ha Y-J, Kim K-H, Cho S-K, Park D-M, Laskowski W, Eskilsson C, Ricchiuto M, Engsig-Karup A P, Cheng, Zheng L, Gu H and Li G, A Comparative Study on the Nonlinear Interaction Between a Focusing Wave and Cylinder Using State-of-the-art Solvers: Part A. *Int. J. Offshore Polar Eng.* 31 (01): 1–10.
- ~~101-102.~~ [Sriram, V., Ma, Q. W. \(2010\). Simulation of 2D breaking waves by using improved MLPG_R method, in: Proceedings of 20th International Offshore and Polar Engineering Conference, Beijing, China, vol. 3: 604–610.](#)
- ~~102-103.~~ [Sriram, V., Ma, Q. W., Schlurmann, T. \(2014\). A hybrid method for modelling two dimensional non-breaking and breaking waves. *J. Comput. Phys.* 272: 429–454.](#)
- ~~103-104.~~ [Sriram, V., Ma, Q.W. \(2012\). Improved MLPG_R method for simulating 2D interaction between violent waves and elastic structures. *J. Comput. Phys.* 231:7650–7670.](#)
- ~~104-105.~~ [Sriram, V., Sannasiraj, S. A., Sundar, V. \(2006\). Numerical simulation of 2D sloshing waves due to horizontal and vertical random excitation. *Applied Ocean Research.* 28\(1\):19-32.](#)
- ~~105-106.~~ [Sriram, V., Sannasiraj, S. A., Sundar, V. \(2006\). Simulation of 2-D nonlinear waves using finite element method with cubic spline approximation. *Journal of Fluids and Structures.* 22\(6\): 663-681.](#)
- ~~106-107.~~ [Sueyoshi M., Kihara H., and Kashiwagi M. \(2007\) A hybrid technique using particle and boundary-element methods for wave-body interaction problems, 9th International conference on numerical ship hydrodynamics, Ann Arbor, Michigan.](#)
- ~~107-108.~~ [Sun, PN, Luo, M, Le Touzé, D and Zhang, AM, 2019d. The suction effect during freak wave slamming on a fixed platform deck: Smoothed particle hydrodynamics simulation and experimental study. *Physics of Fluids.* 31 \(11\), 117108.](#)
- ~~108-109.~~ [Vacondio R, Altomare C, De Leffe M , Hu X, Le Touz D, Lind S, Marongiu J C , Marrone S , Rogers B.D., Iglesias A S \(2020\). Grand challenges for Smoothed Particle Hydrodynamics numerical schemes. *Computational Particle Mechanics*, 8:575–588](#)
- ~~109-110.~~ [Vacondio, R., Rogers, B. D., Stansby, P. K., Mignosa, P. and Feldman, J. \(2013\). Variable resolution for SPH: A dynamic particle coalescing and splitting scheme, *Computer Methods in Applied Mechanics and Engineering.* 256: 132–148.](#)
- ~~110-111.~~ [Verbrugge, T, Domínguez, JM, Crespo, AJC, Altomare, C, Stratigaki, V, Troch, P and Kortenhaus, A, 2018. Coupling methodology for smoothed particle hydrodynamics modelling of non-linear wave-structure interactions. *Coastal Engineering.* 138, 184-198.](#)
- ~~111-112.~~ [Violeau D, Rogers BD. \(2016\) Smoothed particle hydrodynamics \(SPH\) for free-surface flows: past, present and future. *J. Hydraul. Res.* 54, 1–26. \(doi:10.1080/00221686.2015.1119209\).](#)
- ~~112-113.~~ [Wall, A. W, Genkinger, S., Ramm, E. \(2007\). A strong coupling partitioned approach for fluid-structure interaction with free surfaces. *Comput. Fluids* 36:169–183.](#)
- ~~113-114.~~ [Y. Zhou and Q. W. Ma \(2018\). A New Interface Identification Technique Based on Absolute Density Gradient for Violent Flows. *Computer Modeling in Engineering and Sciences.* 115 \(2\) :137-147.](#)
- ~~114-115.~~ [Yan S, Ma QW, Wang J \(2020\), ‘Quadric SFDI for Laplacian Discretisation in Lagrangian Meshless Methods’, *Journal of Marine Science and Application*, 19:362–380.](#)
- ~~115-116.~~ [Yan, R, Monaghan, JJ, Valizadeh, A and Xu, F, 2015. The effect of air on solid body impact with water in two dimensions. *Journal of Fluids and Structures.* 59, 146-164.](#)
- ~~116-117.~~ [Yan, S. and Ma, Q. W. \(2007\). Numerical simulation of fully nonlinear interaction between steep waves and 2D floating bodies using the QALE-FEM method.](#)

Journal of Computational Physics. 221:666–692.

- ~~117-118.~~ Yan, S., Ma, Q. W. (2007). Numerical simulation of fully nonlinear interaction between steep waves and 2D floating bodies using the QALE-FEM method. *J Comput Phys.*221:666-692.
- ~~118-119.~~ Yan, S., Ma, Q. W. and Cheng, X. (2011). Fully nonlinear hydrodynamic interaction between two 3d floating structures in close proximity. *International Journal of Offshore and Polar Engineering.* 21:178–185.
- ~~119-120.~~ Yang, Q, Xu, F, Yang, Y and Wang, J, 2020. Two-phase SPH model based on an improved Riemann solver for water entry problems. *Ocean Engineering.* 199, 107039.
- ~~120-121.~~ Ye T, Pan D, Huang C, Liu MB. (2019) Smoothed particle hydrodynamics (SPH) for complex fluid flows: recent developments in methodology and applications. *Phys. Fluids* 31, 011301. (doi:10.1063/1.5068697).
- ~~121-122.~~ Zhang N, Yan S, Zheng X, Xu G, Ma Q W (2021), ‘Numerical Study of Interaction of Focused Waves with a Fixed Cylinder by a Hybrid Model Coupling SPH and QALE-FEM’, *International Journal of Offshore and Polar Engineering* 31(1):45-52.
- ~~122-123.~~ Zhang N, Zheng X, Ma Q (2019), ‘Study on wave-induced kinematic responses and flexures of ice floe by Smoothed Particle Hydrodynamics’, *Computers and Fluids* 189:46-59.
- ~~123-124.~~ Zhang, A, Sun, P and Ming, F, 2015. An SPH modeling of bubble rising and coalescing in three dimensions. *Computer Methods in Applied Mechanics and Engineering.* 294, 189-209.
- ~~124-125.~~ Zhang, N., Xing Z, Ma Q.W, Hu Z, (2019), “A numerical study on ice failure process and ice-ship interactions by Smoothed Particle Hydrodynamics”. *International Journal of Naval Architecture and Ocean Engineering*, 2019,11(2):796-808.
- ~~125-126.~~ Zhang, Y and Wan, D, 2018. MPS-FEM coupled method for sloshing flows in an elastic tank. *Ocean Engineering.* 152, 416-427.
- ~~126-127.~~ Zheng, X, Ma, QW and Duan, WY, 2014. Incompressible SPH method based on Rankine source solution for violent water wave simulation. *Journal of Computational Physics.* 276, 291-314.
- ~~127-128.~~ Zhou Y., and Dong P (2018). A new implementation method of sharp interface boundary conditions for particle methods in simulating wave interaction with submerged porous structure. *Computers & Fluids.*177:87-100.
- ~~128-129.~~ Zhou, B. Z., Wu, G. X. and Teng, B. (2015). Fully nonlinear wave interaction with freely floating non-wall-sided structures. *Engineering Analysis with Boundary Elements.* 50:117–132.
- ~~129-130.~~ Zhou, J. T, Ma, Q. W. (2010). MLPG method based on Rankine source solution for modelling 3D breaking waves. *CMES.* 56(2):179–210.
- ~~130-131.~~ Zhou, J. T. (2010). Numerical investigation of breaking waves and their interactions with structures using MLPG_R method. PhD Thesis, School of Engineering and Mathematical Sciences, City, University of London.
- ~~131-132.~~ Zhou, J. T., Ma, Q. W., Yan, S. (2008) Numerical Implementation of Solid Boundary Conditions in Meshless Methods. *Proceedings of the Eighteenth (2008) International Offshore and Polar Engineering Conference.* 8:16–23.
- ~~132-133.~~ Zhou, Y., Ma, Q. W., Yan, S. (2017). MLPG_R method for modelling 2D flows of two immiscible fluids. *International Journal for Numerical Methods in Fluids.* 84:385–408.

[133-134.](#) Zhou, J. T, Ma, Q. W. Yan S. (2008). Numerical Implementation of Solid Boundary Conditions in Meshless Methods, Proceedings of the Eighteenth (2008) International Offshore and Polar Engineering Conference, 16-23.